# THE CHARACTERISTICS OF Mb 4.9 TURKANA RIFT MAINSHOCK-AFTERSHOCKS SEQUENCE, EAST AFRICA.


**PRESENTED**
**BY**
**SAMUEL MWANGI NDERITU**

# Introduction: Background Information

**What are aftershocks?**

Aftershocks are typically smaller earthquakes that occur after the mainshock and they follow certain spatial and temporal windows (Liu & Stein, 2011; Yukutake & Lio, 2017).

**What are Epidemic Type of Aftershocks?**

In Epidemic Type of Aftershocks;

- Mainshock produce offspring earthquakes and the offspring earthquakes produce other offspring earthquakes and so on.
- Earthquakes are events characterized by occurrence time, location, and magnitude (Wessel et al., 2019).

**How do Epidemic Type of Aftershocks occur?**

Mainshock trigger the perturbation of the state of stress in some area around it.

These zones of perturbation intersect in time and space and each event can be considered as an offspring of all preceding events (Baranov et al., 2019).

# Background Information Cont'd

**What is Epidemic Type of Aftershocks Sequence (ETAS) model?**

The ETAS model is a point process representing the activity of earthquakes of magnitude, Mc, and larger in a region for a given period, where Mc is the cut-off magnitude (Ogata, 1998).

In ETAS model, earthquake occurrences are modeled as cascades; the Poissonian earthquakes produced by the tectonic loading of the area trigger the first generation of aftershocks and so on (e.g., Wessel et al., 2019).

**Why are these Aftershocks important?**

Occurrence of the epidemic type of aftershocks is related to Omori's Law. This is used to develop statistical models for assessing probabilistic time-dependent destructive events after each mainshock (e.g., Gerstenberger et al., 2005).

# Background Information Cont'd

## What is Omori's Law?

The rate of occurrence of the aftershocks decreases with time and following Omori's principle (Omori, 1894; Utsu, 1961; Liu & Stein, 2011) determined by (Equation 1):

$$n(t) = \frac{K}{(c+t)^p} \qquad \text{(Ogata, 2006)} \qquad \text{(Equation 1)}$$

- Where:
- **n (t)** is the number of aftershocks by time, **t**
- **K** is a constant and a positive number and depends strongly on cut-off magnitude
- **c** is a constant and a positive number close to zero
- **p** is a constant and a positive number close to one.

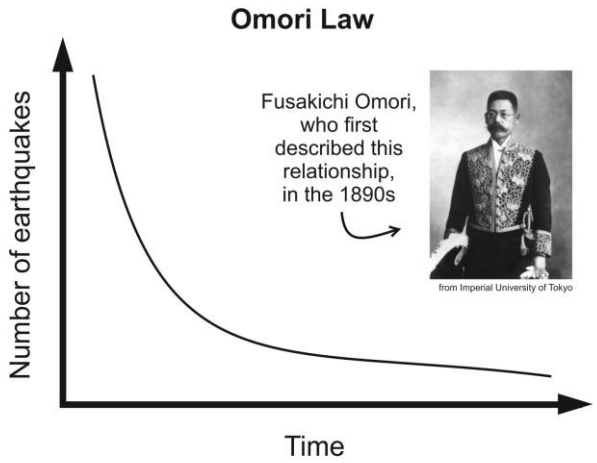

# Background Information Cont'd

**ETAS Statistical Model**

The rate of aftershocks occurrence at time **t** following the **$i^{th}$** earthquake (time; **$t_i$**, magnitude; **$M_i$**) is given by;

$$n_i(t) = K \exp[\alpha(M_i - M_c)] / (t - t_i + c)^p \text{ , For } t > t_i \quad \text{(Ogata, 2006)} \quad \text{(Equation 2)}$$

where $K, \alpha, c,$ and $p$ are constants, that are common to all aftershock sequences in the region.

The rate of occurrence of the sequence at time, **t,** becomes:

$$\lambda(t) = \mu + \sum_i n_i(t) \quad \text{(Ogata, 2006)} \quad \text{(Equation 3)}$$

# Objectives

The objectives of the study are to:

- Determine the main rupture plane and the subsidiary minor faults from the fault plane solutions of the mainshock and large aftershocks.
- Develop an improved statistical model for assessing earthquake hazards in the Turkana region.
- Undertake comparative analysis of the structural and rheological characteristics of the 2014 $M_w$5.2 Karonga and the Mb4.9 Turkana earthquake sequences.

# Literature Review: Tectonic Setting

(a)

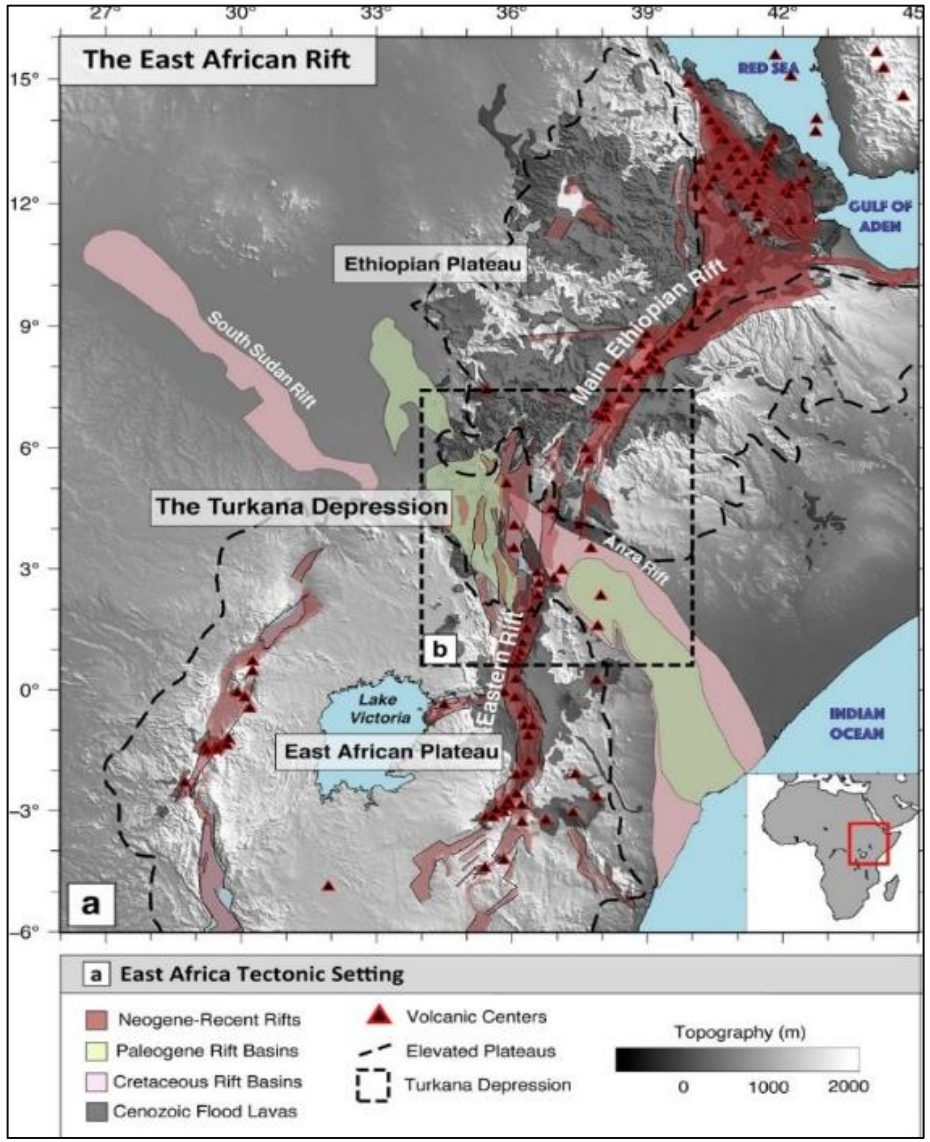


(b)

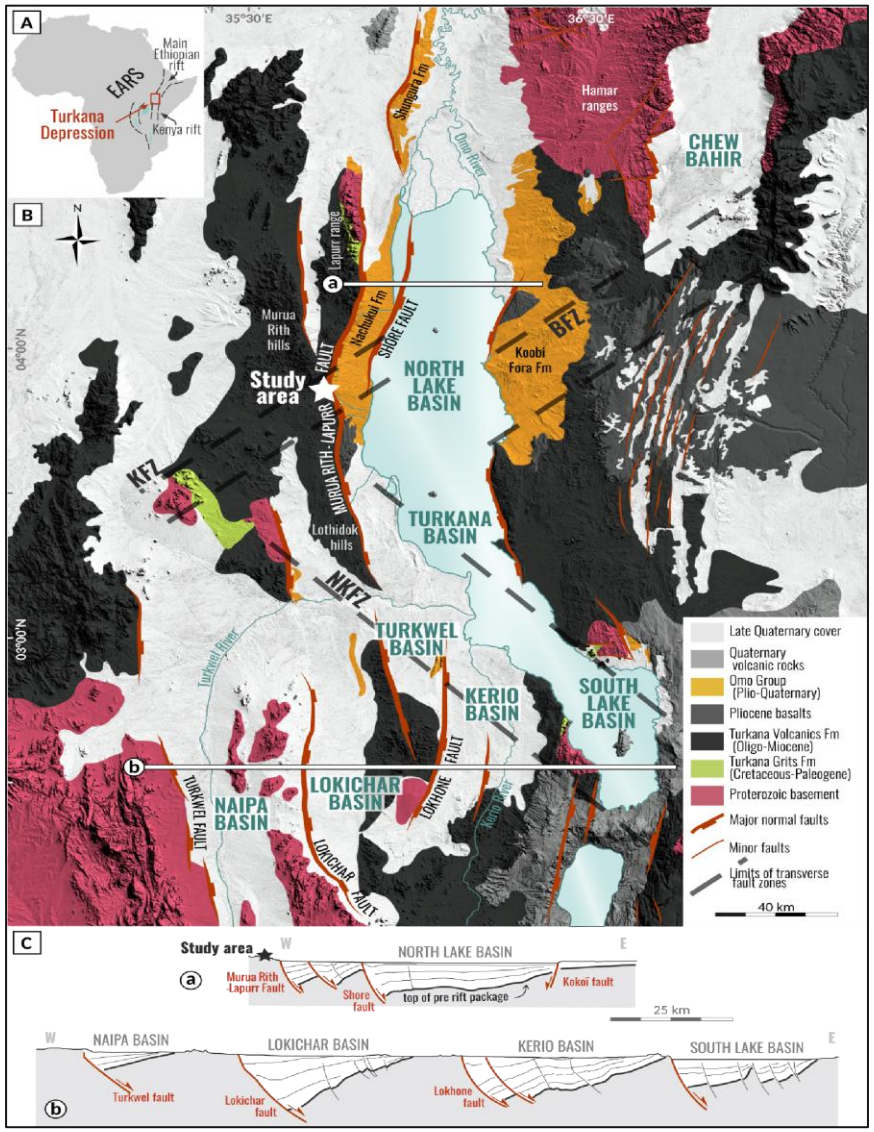


(a) Interaction of MER, EAR and Kino Sogo fault belt in the Turkana Depression (Kounoudis et al., 2021).

(b) Structural and geological background of the Turkana Depression (Ragon et al., 2018).

# Literature Review : Geophysical Background

Several geophysical studies have been carried out in Turkana Depression and EARS at large. KRISP, (e.g., Prodehl et al., 1994; KRISP Working Group., 1994), through wide-angle reflection studies determined crustal thickness variations and uppermost mantle structure of the EARS. They reveal a crustal thickness of ~35km beneath the East African plateau and ~20km beneath Lake Turkana. [Musila et al., Submitted, 2022] modifies KRISP [1991] 1-D velocity model that stabilizes to depths of up to ~25km, coinciding with the Moho boundary beneath some areas and lower crust elsewhere. A 1.75 $V_p/V_s$ ratio for the local events is also determined in the new velocity model.

Kounoudis et al., [2021] reveal low wavespeed anomalies ($^{\delta}V_p$ = -1.5%, $^{\delta}V_s$ = -2.5%) in the uppermost mantle beneath L. Turkana across the region towards the mantle-transition zone depths. The low wavespeeds corroborate with recent Pleistocene and Holocene volcanic centres at <150 km depth. Evidence of an elongated high wavespeed anomaly at ~$5^0$ N ($^{\delta}V_p$ = 1.5%) is determined and traverses NW-SE southern Ethiopia to <200 km depth.

# Literature Review : Seismic Background

Earthquake monitoring in Kenya and Africa, in general, remains a concern since the seismic networks are scattered. Currently, there are few permanent seismic stations operated by different institutions and organizations [Bruce, 2013; Mulwa et al., 2014]. The northern part of Kenya has a broadband seismic station, LODK, which is part of the GEOFON seismic network closely monitoring the region despite being an area of interest both tectonically and seismically. [Mulwa et al., 2014] states that the current seismic network in Kenya implies that events with $M_l \leq 3.0$ are only detectable at distances not greater than 350 km from the center of the network.

The general seismicity of the eastern branch of the EARS is moderate while seismicity in the Kenya Rift is relatively low [Ibs-van Seht et al., 2001; Mulwa et al., 2020] while it is higher on the western branch (Lavayssiere et al., 2017; Ebinger et al., 2019) (Fig 5). [Tongue et al., 1994] shows swarm earthquakes with a restricted depth of 5km with sub-vertical fault plane solutions below L. Baringo.

# Literature Review: Seismic Background Cont'd

[Ibs-van Seht et al., 2001] describe the small magnitude events in the eastern branch of the EARS, $M \leq 3$, as swarm earthquakes, which are very common. The largest event in the Turkana Depression was the 1913 $M_s$=6.2 [Ambraseys, 1991; Mulwa et al., 2020]. Other events in the Turkana region are summarized in Figure 5 [Ambraseys, 1991; Mulwa et al., 2014; Musila et al., 2020; Kounoudis et al., 2021].

The general seismicity of Kenya is associated with the Tertiary and Quaternary structures and volcanism [Maguire et al., 1988]. The general depth of earthquakes in the southern part of the Kenya Rift is restricted to 10 km [Young et al., 1991; Ibs-van Seht et al., 2001; Mulwa et al., 2014] while the swarm earthquakes in the central part of the rift are found to form a narrow-elongated cluster at about 5 km depth [Young et al., 1991; Tongue et al., 1994; Mulwa et al., 2014].

Seismicity in the western branch spans 2-35km depth range (Ebinger 2019; Zheng et al., 2020). Study done by Zheng et al., 2020 in Karonga, Malawi, indicate shallow earthquakes caused by both aseismic slip and deep seismic slip characterized by episodes of multiple faulting and fault intersections. Strain is distributed across multiple faults above 12km. The aftershocks of the $M_w$ 5.2 Karonga sequence occurred at fault intersections between only the east dipping and west dipping St. Mary fault, but other shallow faults at 5-to 10-km depth.

# Literature Review: Seismic Background Cont'd

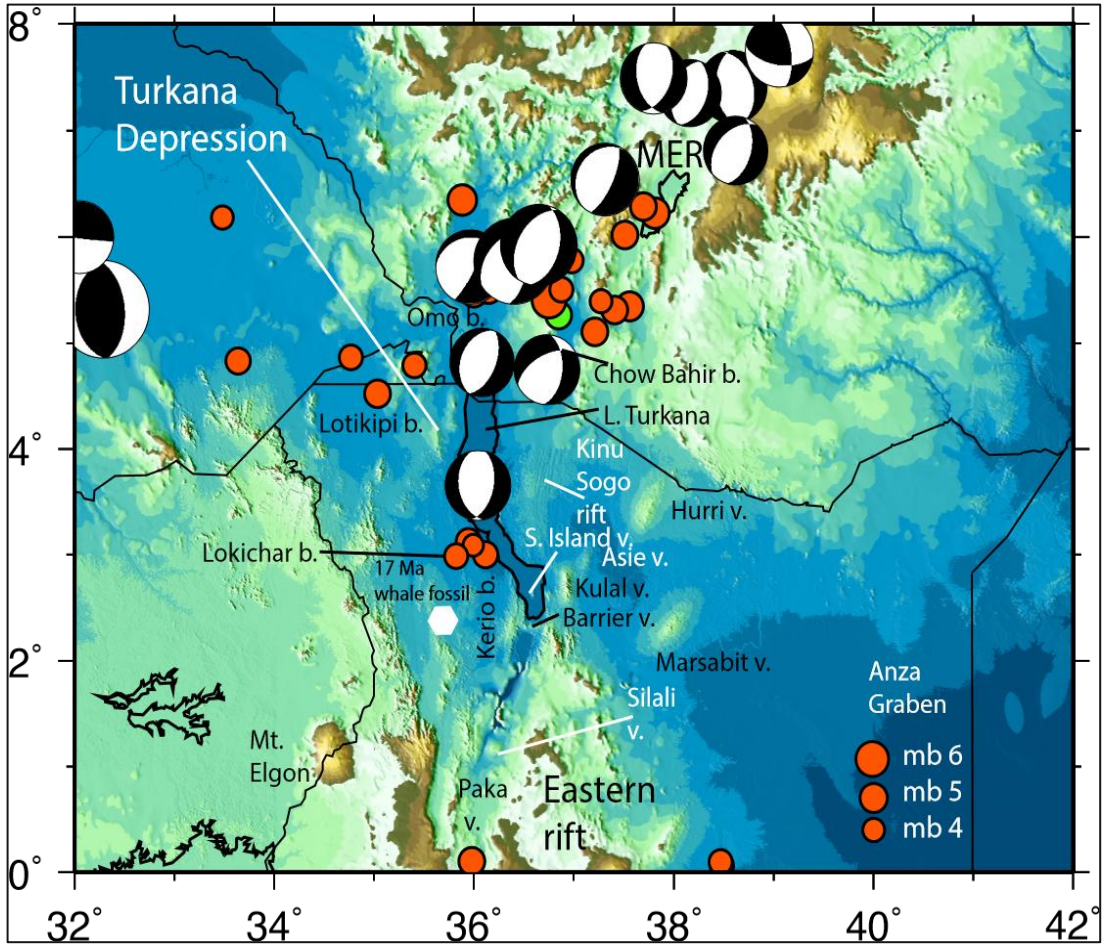


Distribution of teleseismically monitored earthquakes in the Turkana Depression 1973-2017 from NEIC and Global CMTs (From Kounoudis et al., 2021)

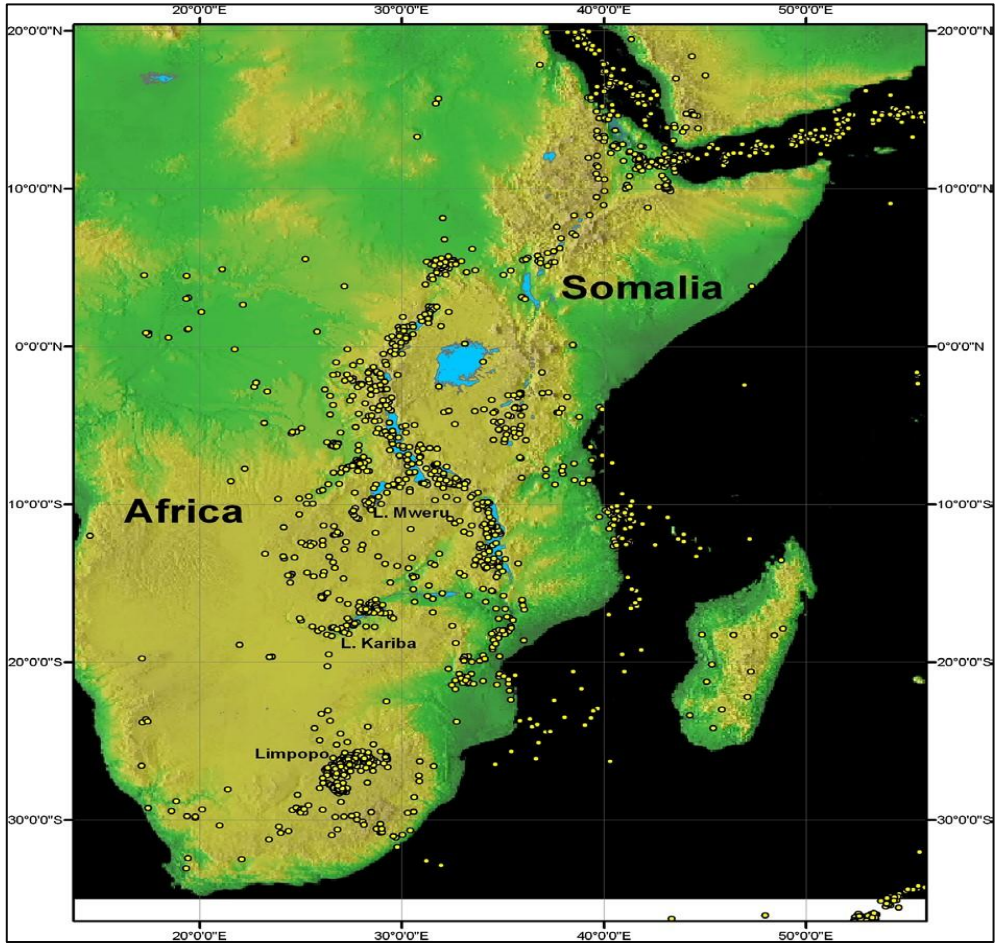


Seismicity of the western and eastern branches of the EARS (From Chorowicz, 2005)

# Literature Review: Seismic Background Cont'd

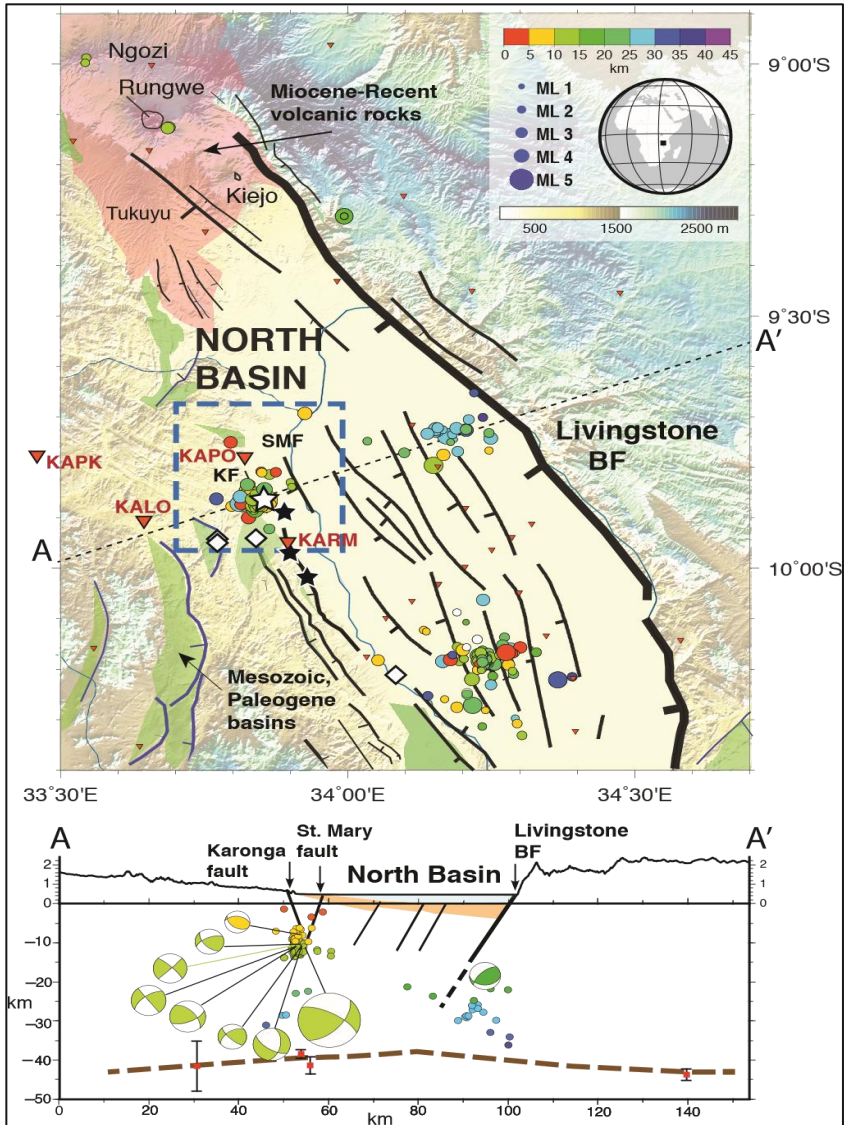


Map of North Basin of the Malawi rift zone. The white star indicates the 2014 $M_w$5.2 Karonga earthquake that occurred in the hanging wall of Livingstone border fault. Inverted triangles are seismic stations. From Ebinger et al., 2019

# Literature Review: Seismic Background Cont'd

The spatial distribution of aftershocks can be mainly classified into 3 different classes (Kisslinger, 1996):

**i. Class 1**

Those that occur on the same section of the main rupture plane or in a narrow zone bordering it around the edges and possibly in thin sheets on both sides. It is assumed that these are the early aftershocks, normally occur between 24 and 48 hours after the mainshock. These are critical in outlining and defining the mainshock rupture plane.

**ii. Class 2**

These occur on the same fault that ruptured to generate the mainshock but are located outside the section of initial slip. They represent the growth of the original aftershock zone.

iii. **Class 3**

These occur on faults other than the fault that produced the mainshock but are presumably triggered by the mainshock. These aftershocks might occur at large distances compared to the dimensions of the mainshock rupture.

# Instrumentation, Data & Methodology

## Instrumentation

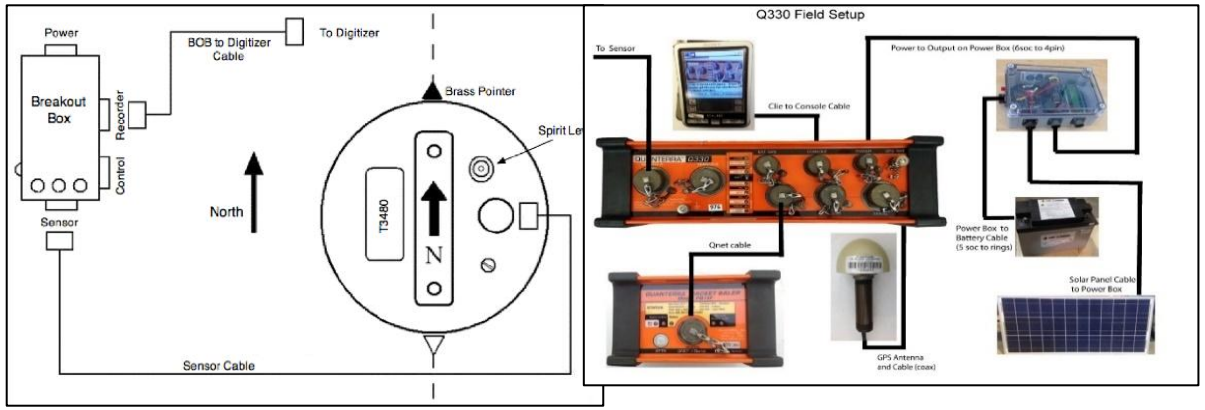


1. ETAS & AFTPOI Programs Written IN FORTRAN Language.
1. R-Module

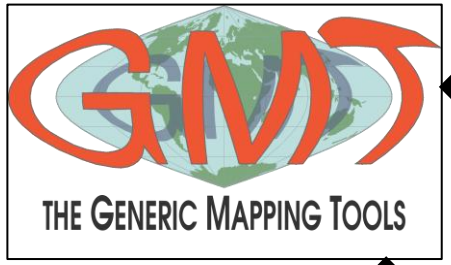


FOCMEC

## Data

The data used is recorded by TRAILS project stations installed in Northern Kenya and Southern Ethiopia regions from January 2019 through June 2021. A total number of 32 temporary seismic stations were installed for this project. The instruments used comprise of CMG-3T sensors, Quanterra (Q330) data loggers and Quanterra Packet Balers for storage.

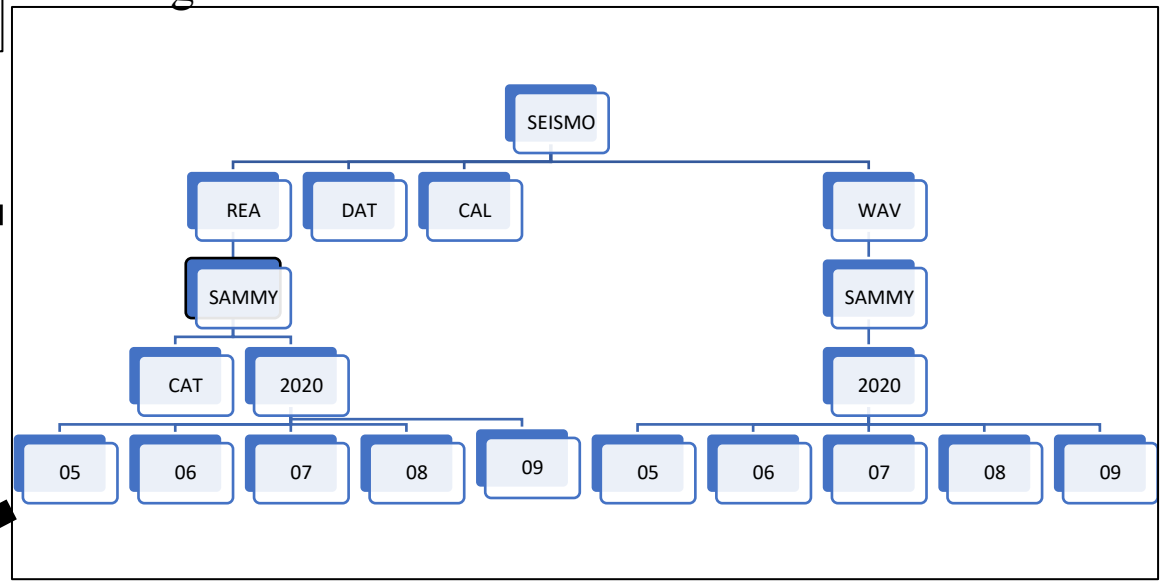

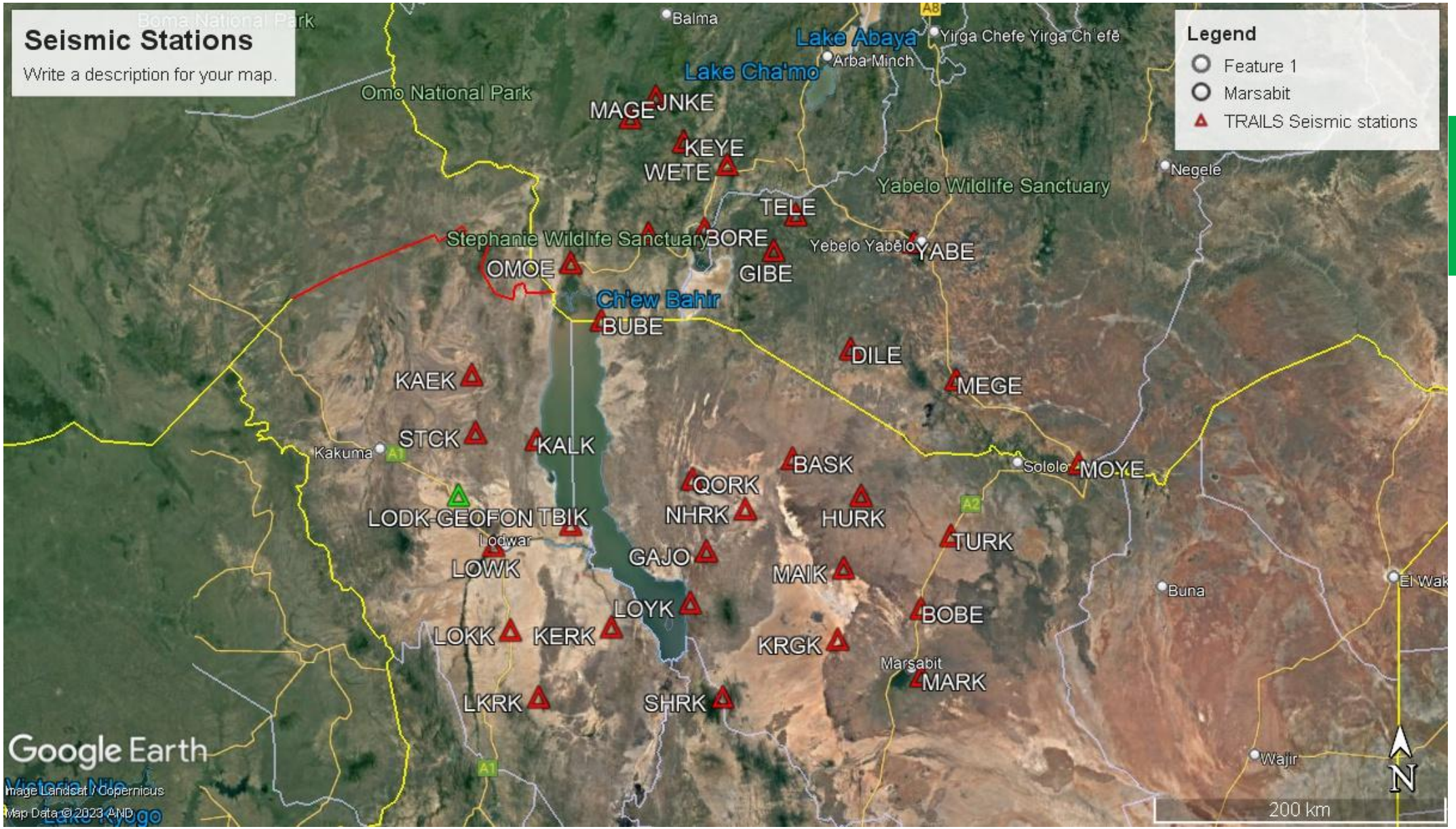


**Trails seismic stations network & LODK GEOFON**

Data collection in North Horr station (NHRK). Photo credit: Sammy (Driver)

# Results And Discussions

# Mainshock Plot in SEISAN

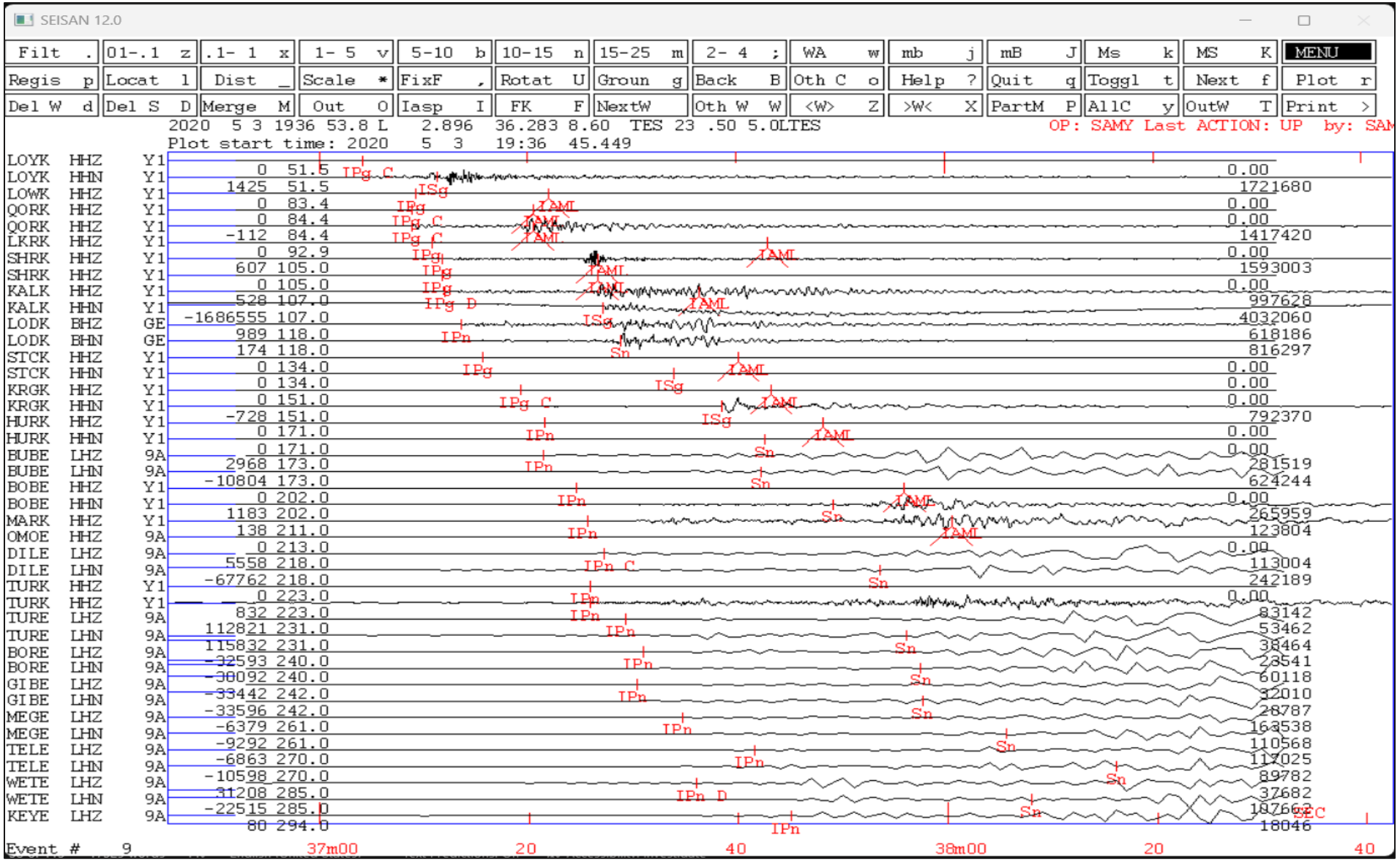


**Mainshock plot in SEISAN: Phase picks, polarities & amplitude peaks**

# Turkana Sequence

**Spatial distribution of the sequence**

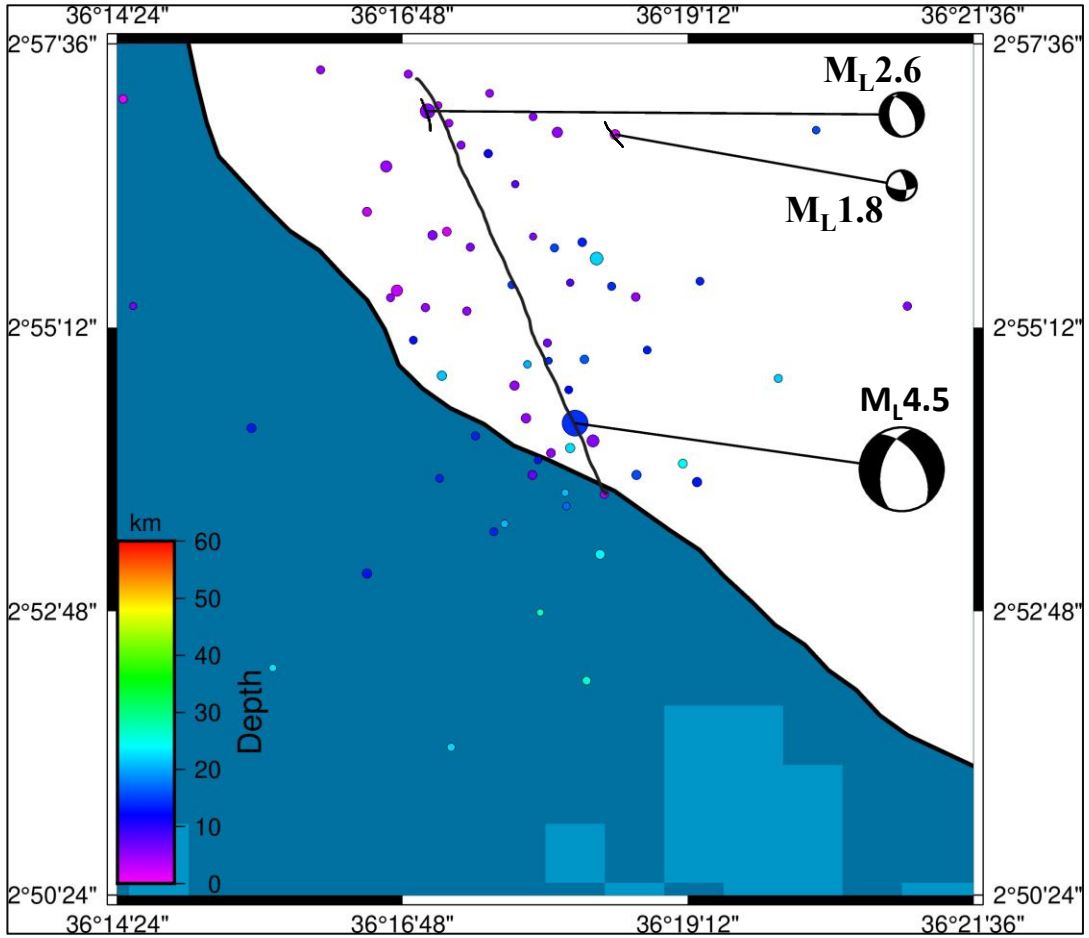


**Time-space distribution of the sequence in days**

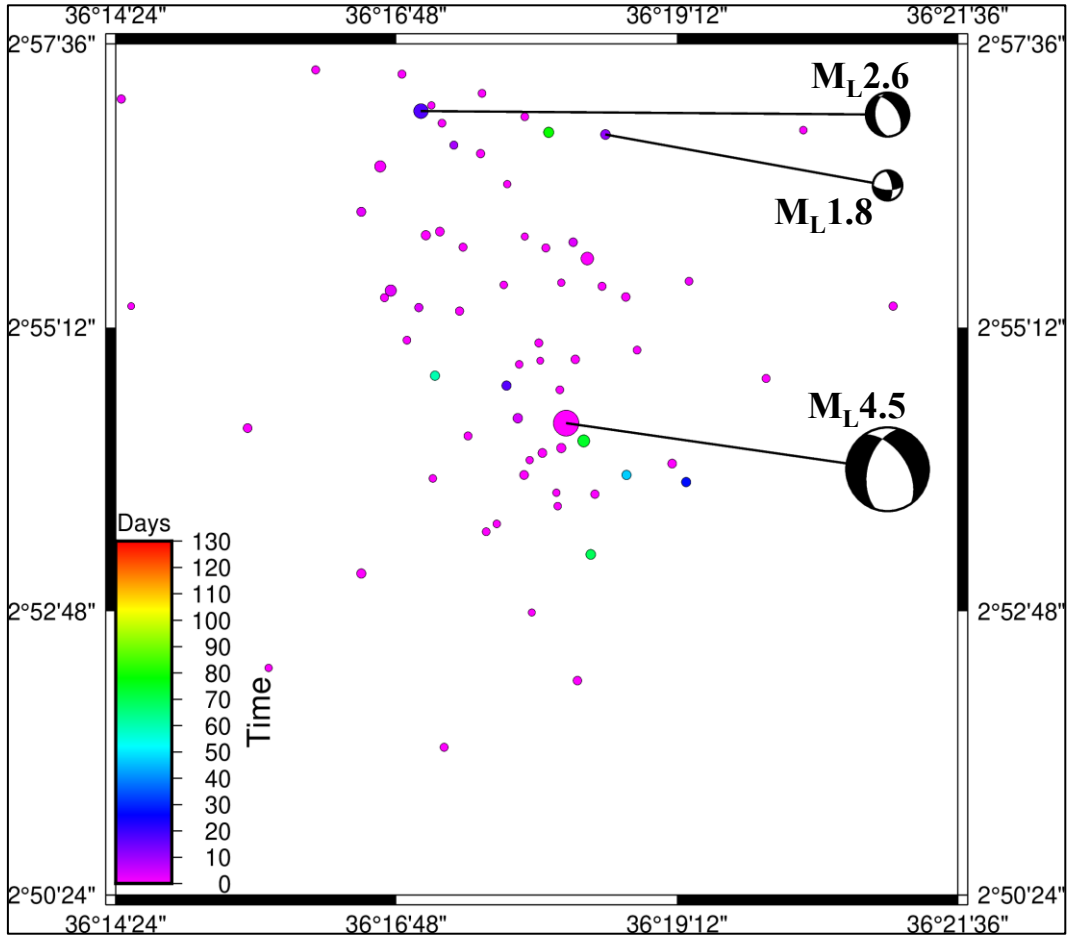

# Focal Mechanisms: Mainshock ($M_L$ 4.5)

**Multiple solutions determined by FOCMEC program using $2^0$ increment.**

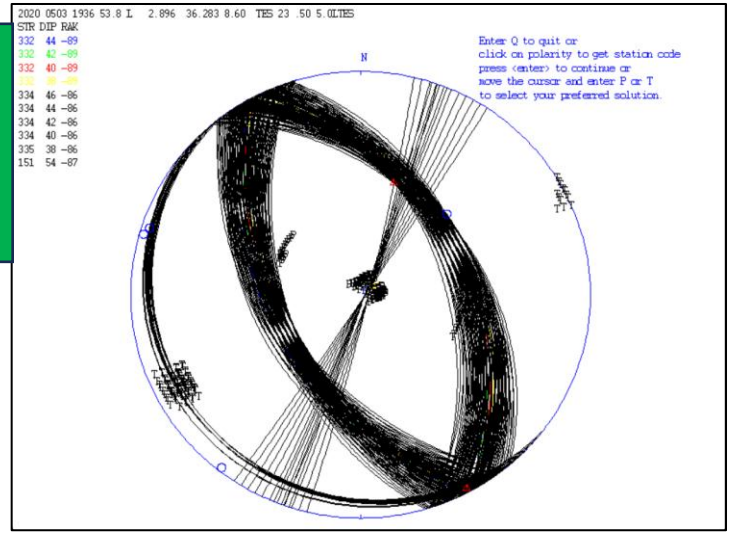


**The three solutions determined by FPFIT, FOCMEC and HASH programs.**

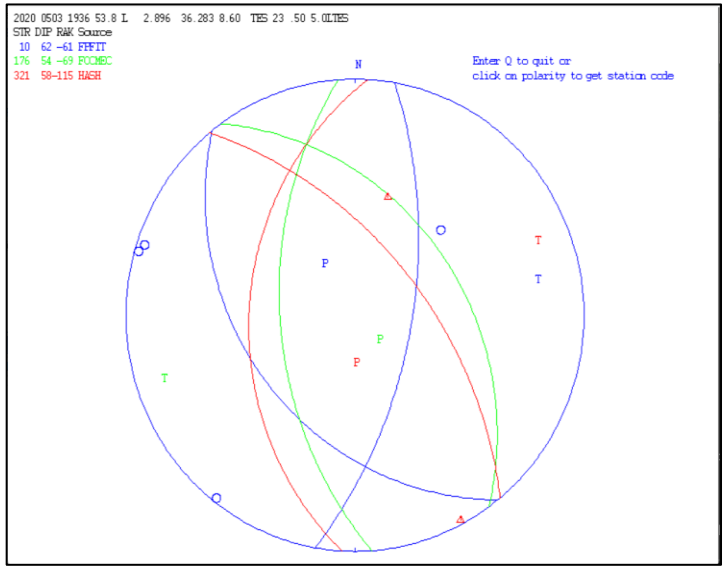


**Best solution determined by FOCMEC program using $16^0$ increment station polarities.**

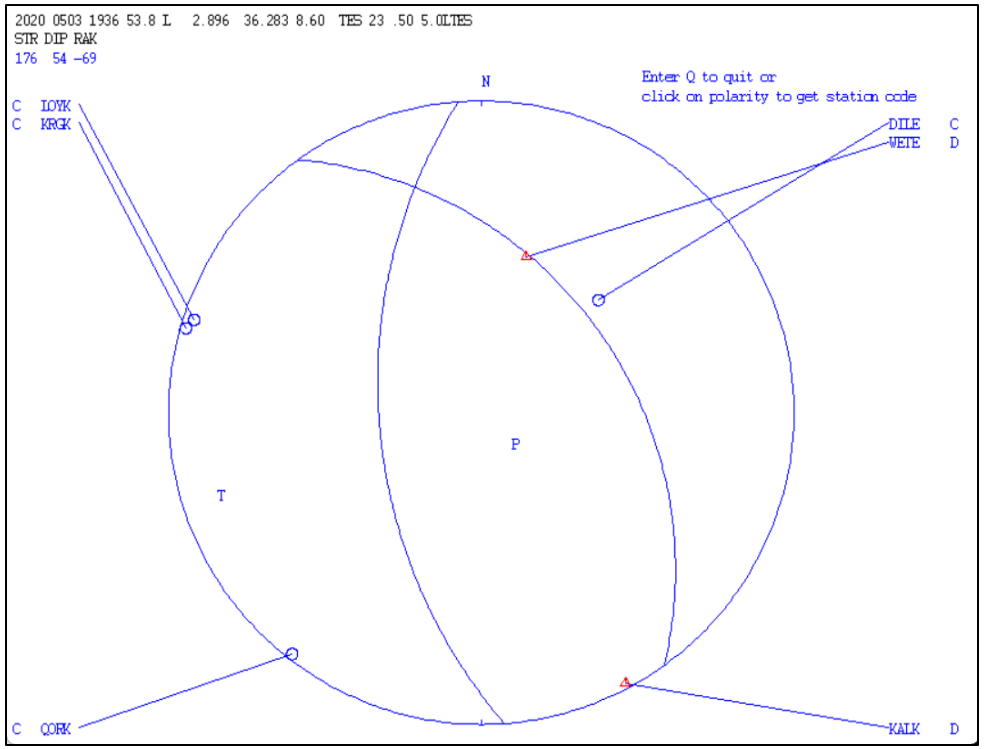

# Turkana Sequence Cont'd

Aftershocks' fault plane solutions:

| Longitude | Latitude | Depth | Strike | Dip | Rake | Magnitude |
|---|---|---|---|---|---|---|
| 36.3098 | 2.9472 | 1.4 | 351.03 | 66.07 | -26.34 | 1.54 |
| 36.2835 | 2.9505 | 5.39 | 176.57 | 42.27 | -67.37 | 2.57 |

# Omori's Law & ETAS Model-Turkana Sequence

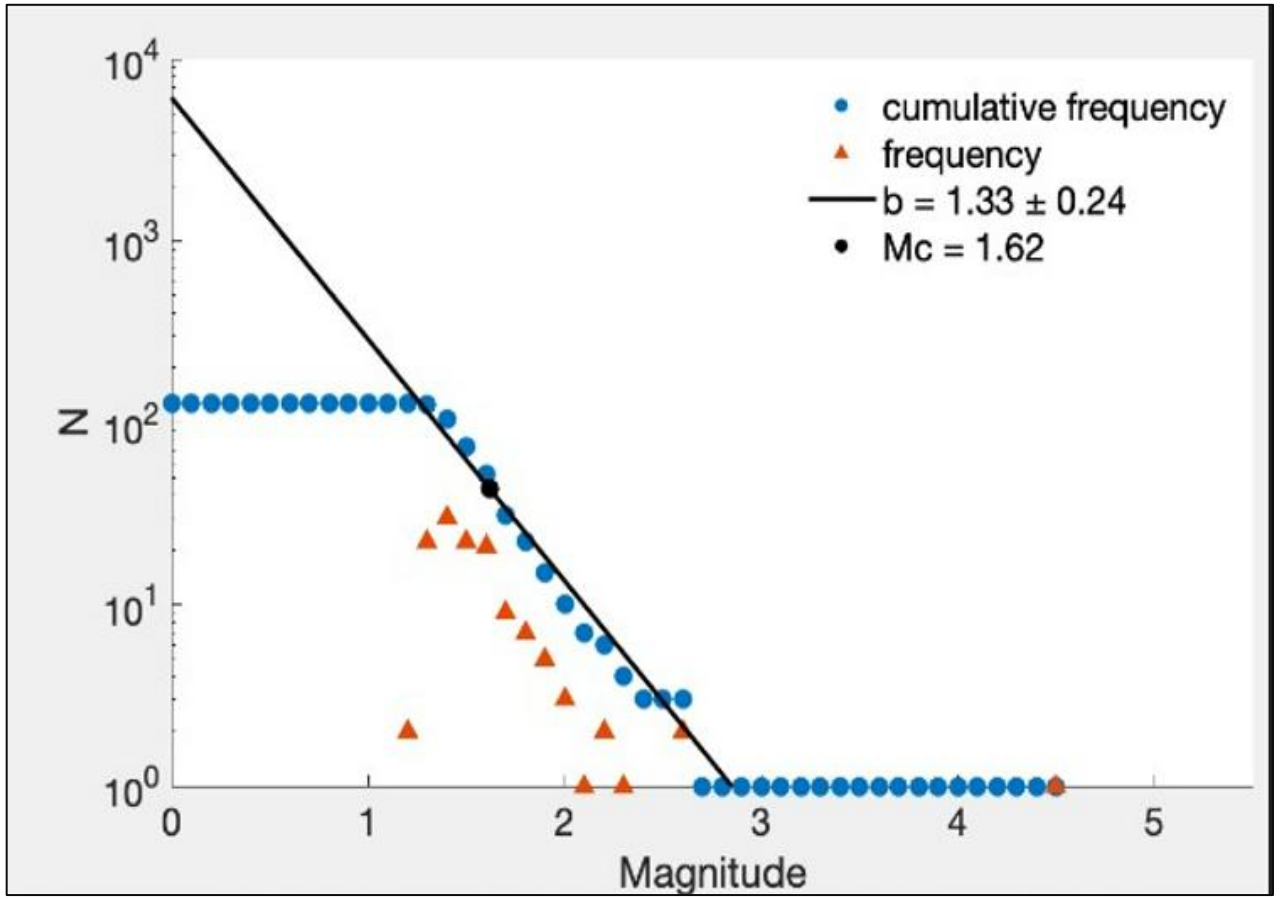


Cut-off magnitude and the b-value

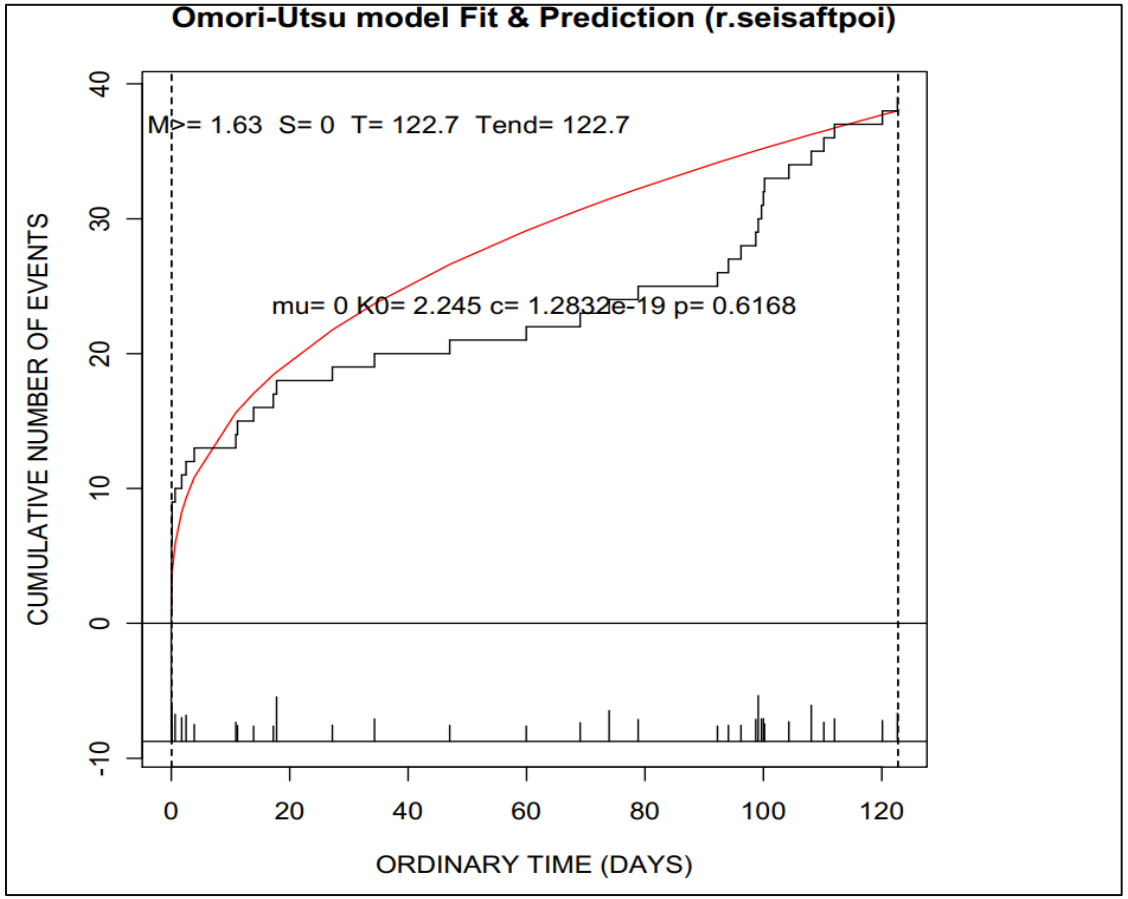


Omori-Utsu/ETAS model fit

# Omori's Law & ETAS Model Cont'd

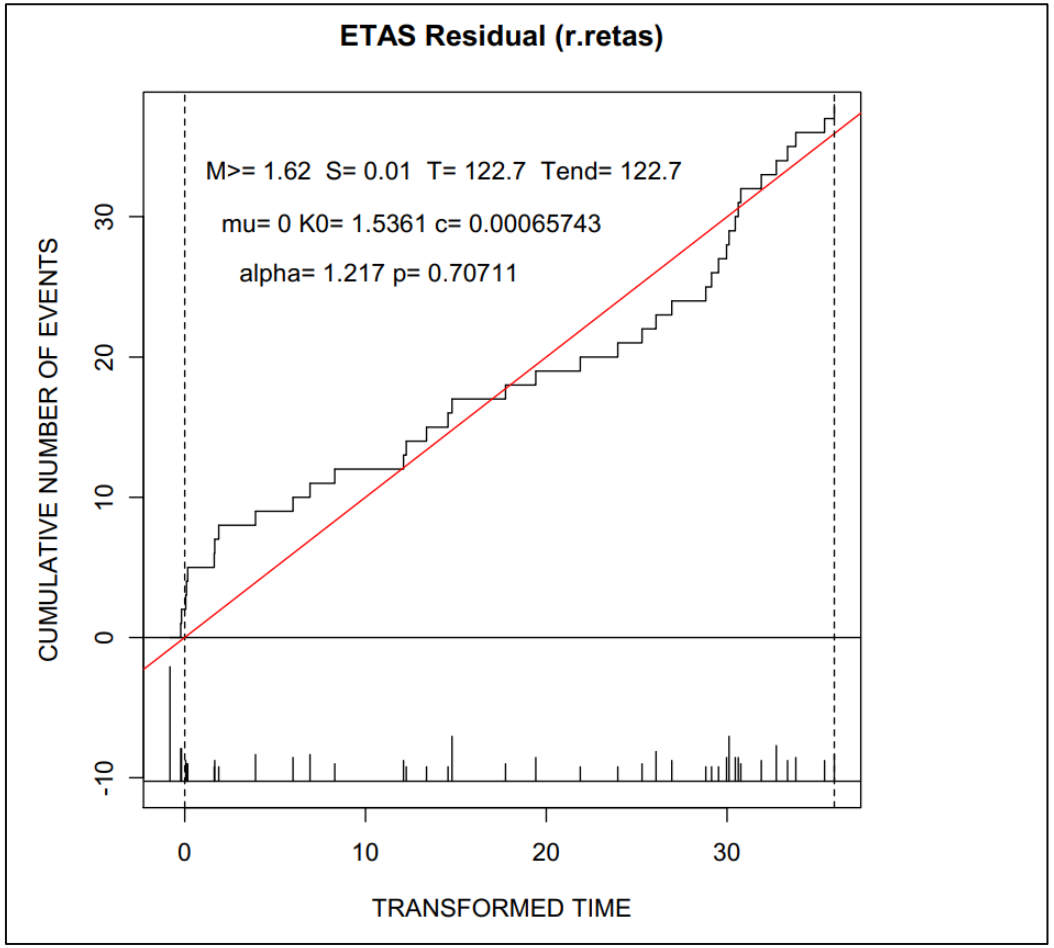


ETAS model cumulative events as a function of transformed time and parameter values

Parameter values and their definition

| Parameter | Definition | Value |
|---|---|---|
| Mc | Cut-off magnitude | 1.62 |
| Tend | Time of the last aftershock | 122.7 (days) |
| S | Start time of the aftershocks | 0.01 (days) |
| mu | Background seismicity | 0 |
| K0 | Positive constant that strongly depends on the Mc | 1.5361 |
| c | Positive constant close to zero | 0.0007 |
| alpha | Efficiency of an earthquake in generating an aftershock | 1.217 |
| p | Rate of decay of the aftershocks | 0.70711 |

# Results: 2014 $M_w$ 5.2 Karonga (Malawi) Sequence

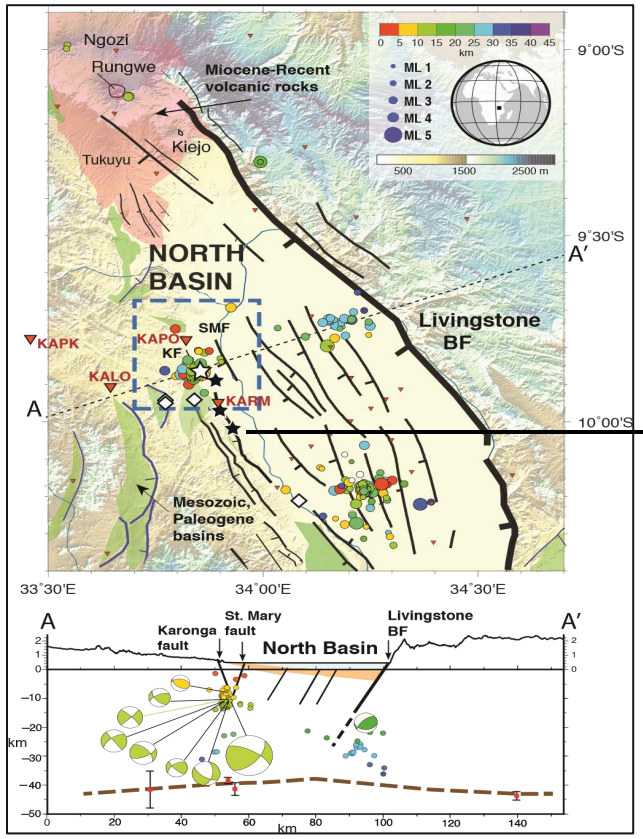


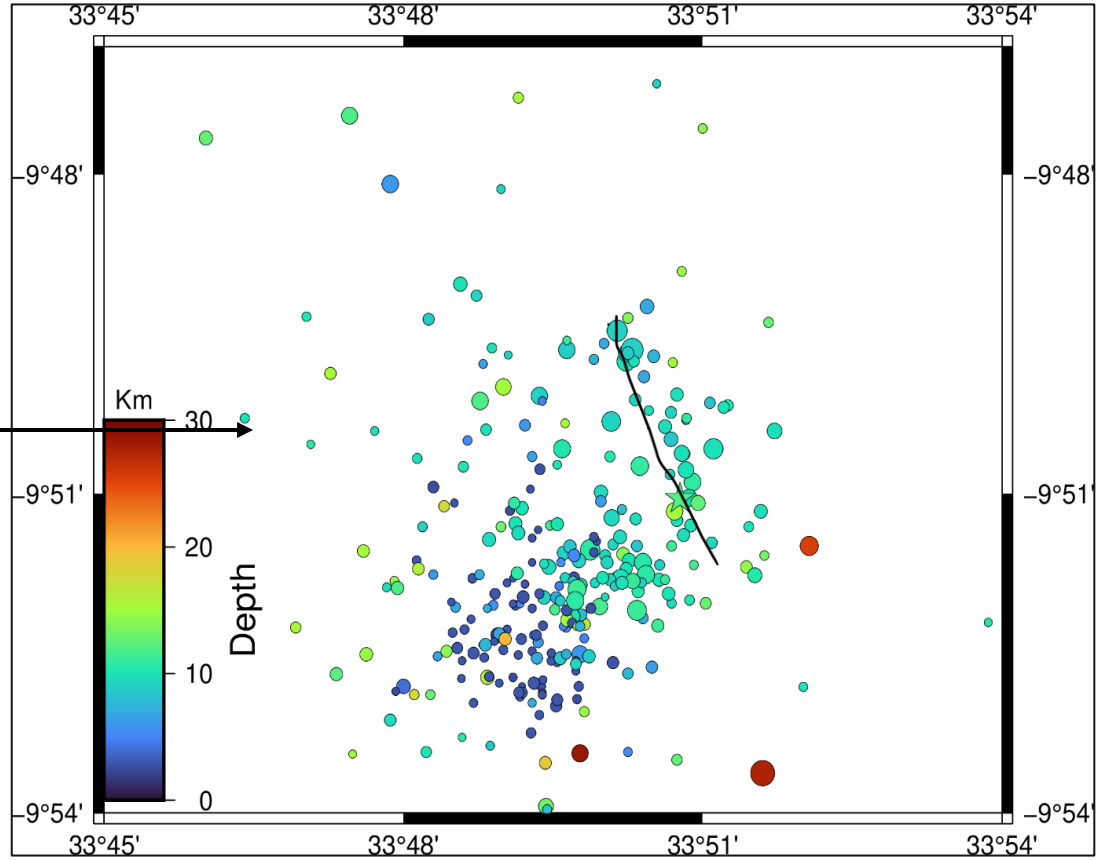


Spatial distribution of the Mw=5.2 Karonga sequence

# Karonga Sequence Cont'd

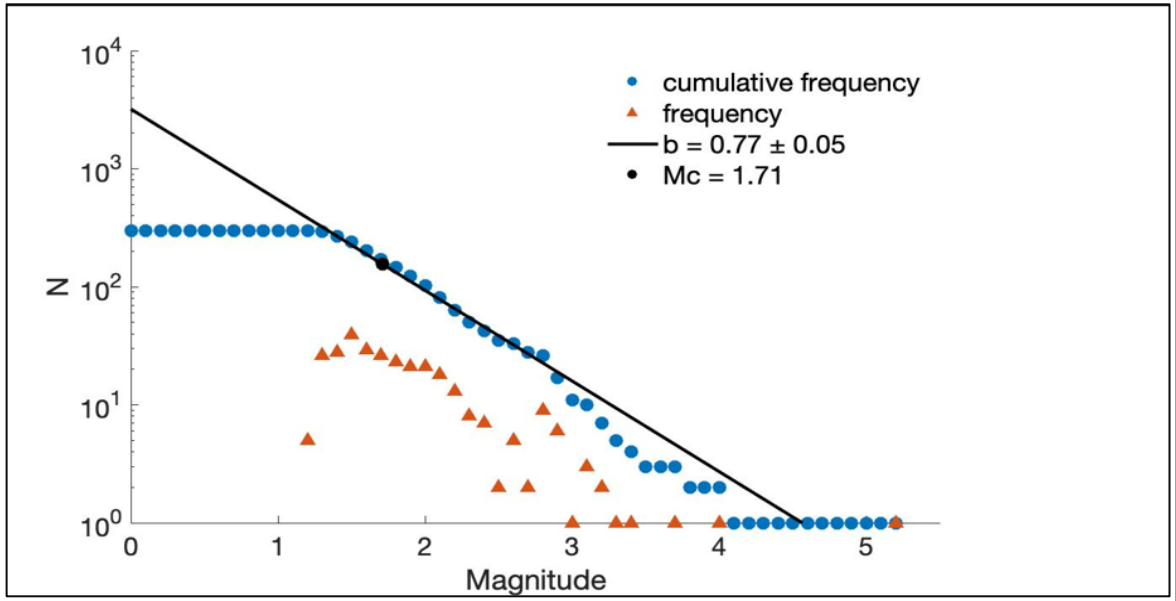


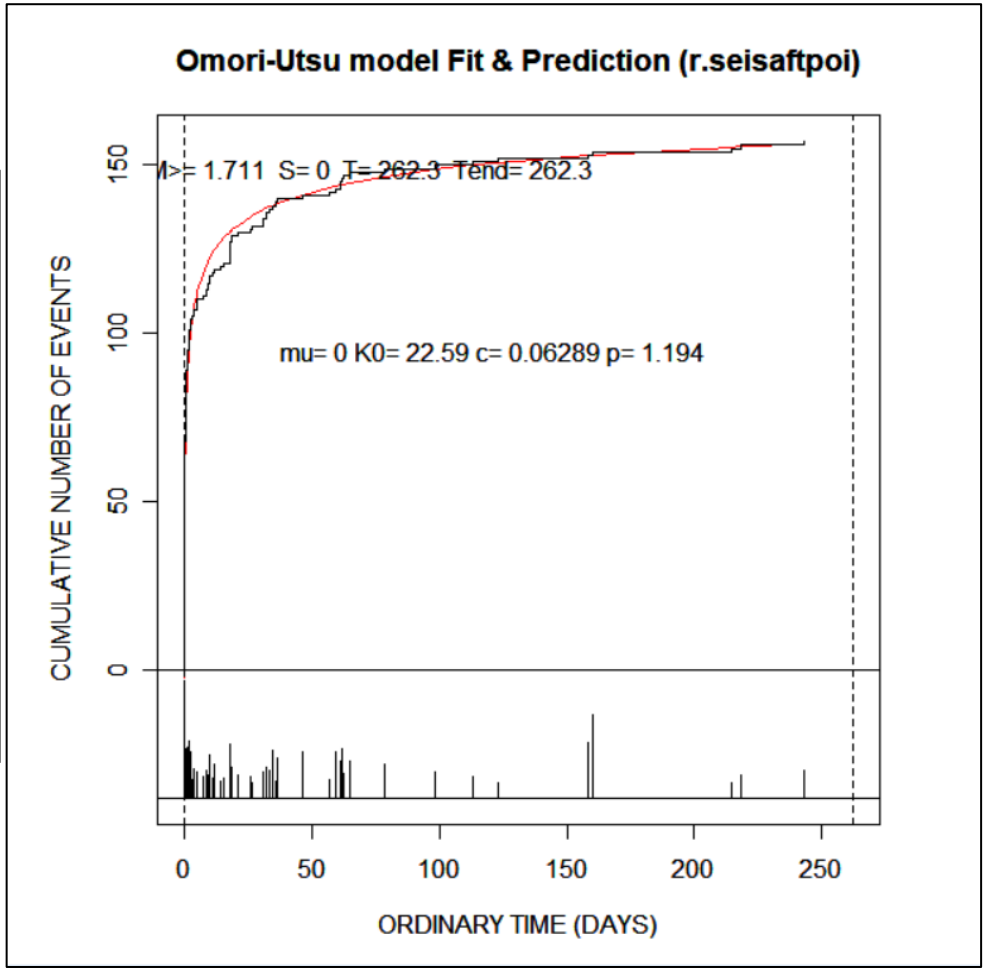


The b-value and cut-off magnitude ($M_c$) for Karonga sequence

# Karonga Sequence Cont'd

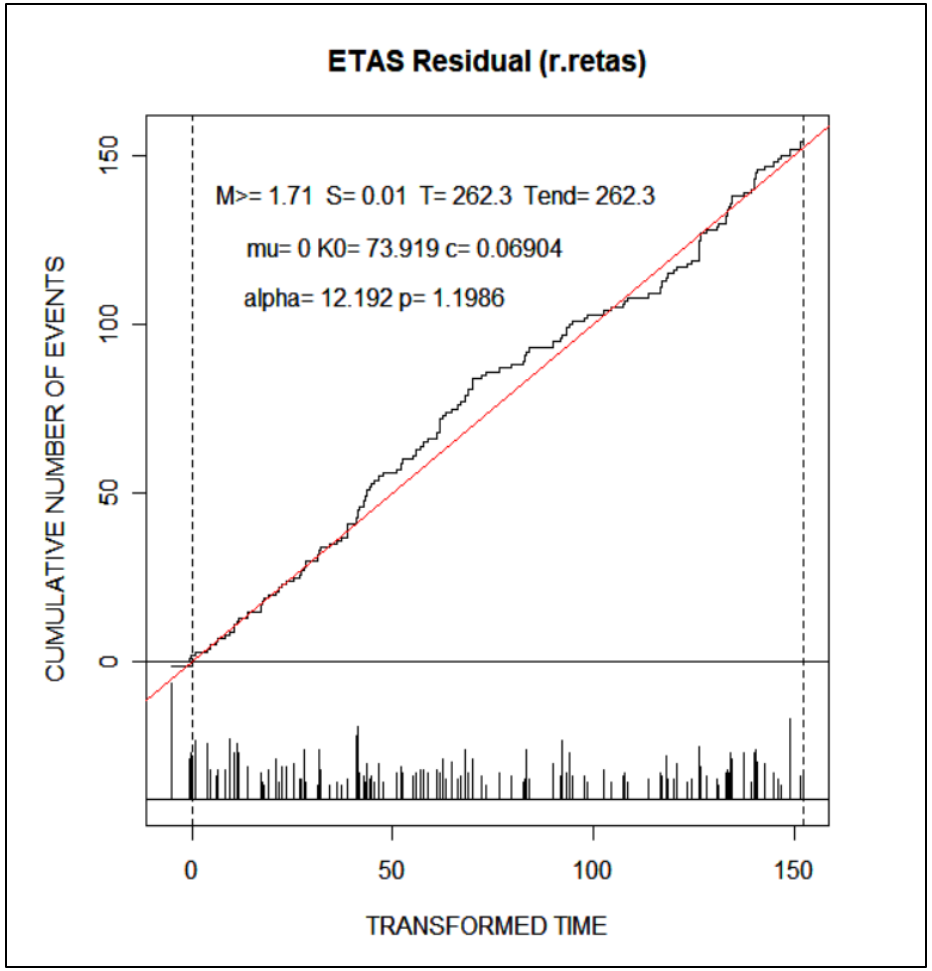


Etas model for the Karonga Sequence

Parameter values and their definition

| Parameter | Value |
|---|---|
| M (cutoff magnitude) | 1.71 |
| Mu | 0 |
| C | 0.069 |
| K0 | 73.919 |
| P | 1.1986 |
| Alpha | 12.192 |

# Turkana-Karonga Comparison

## Turkana Spatial Distribution

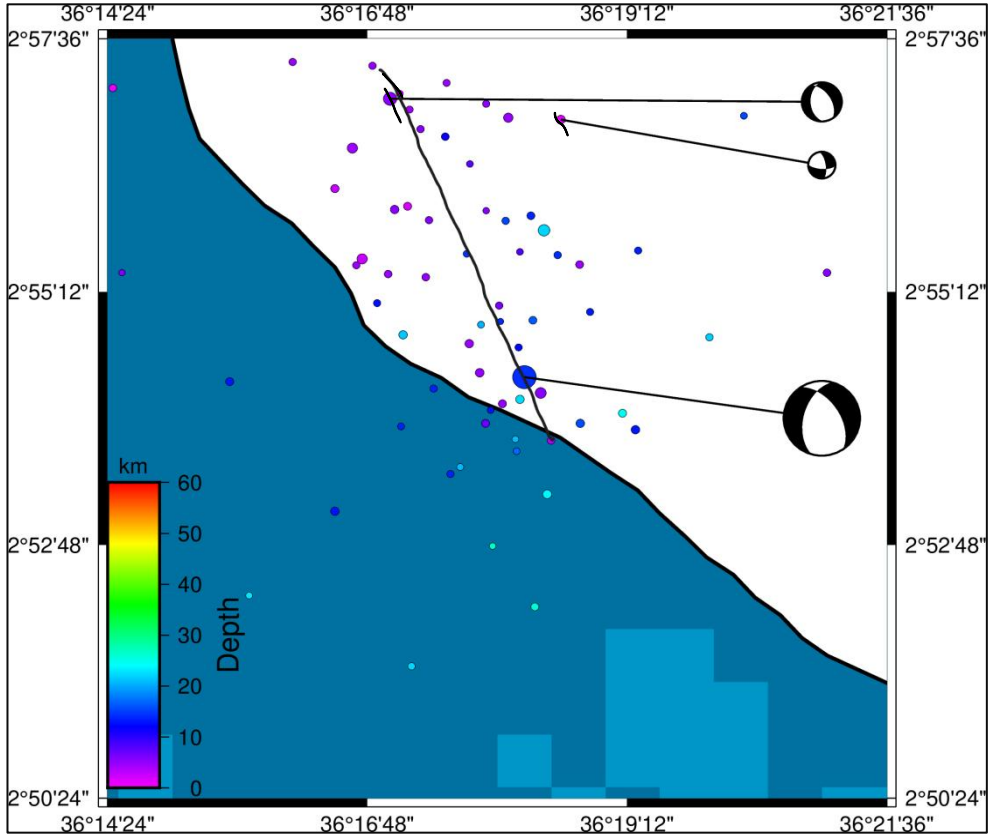


## Karonga Spatial Distribution

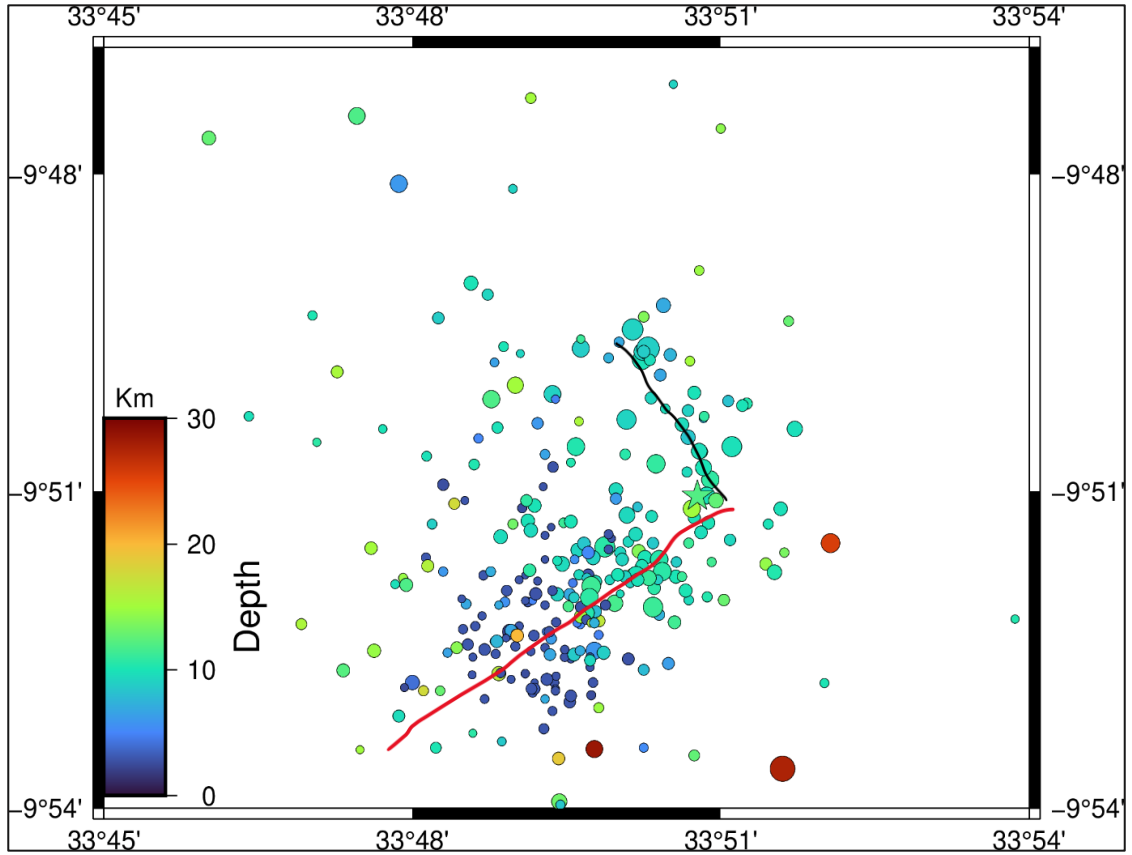

# Turkana-Karonga Comparison

**$M_L$=4.5 Turkana Sequence b-value**

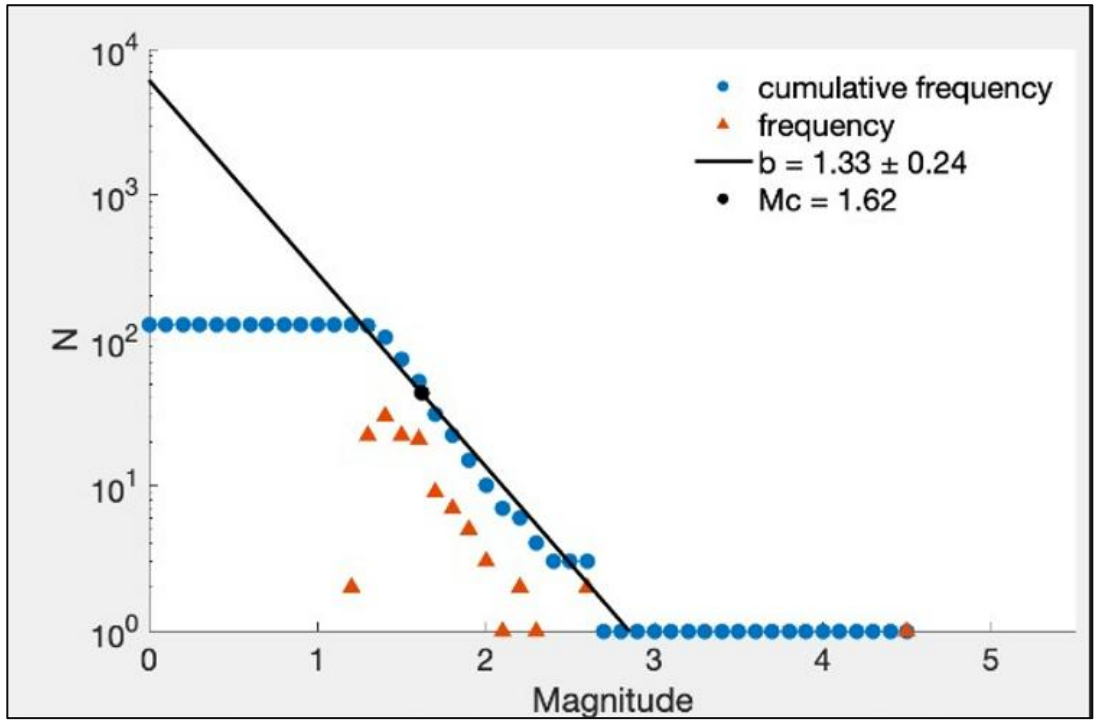


**$M_w$=5.2 Karonga Sequence b-value**

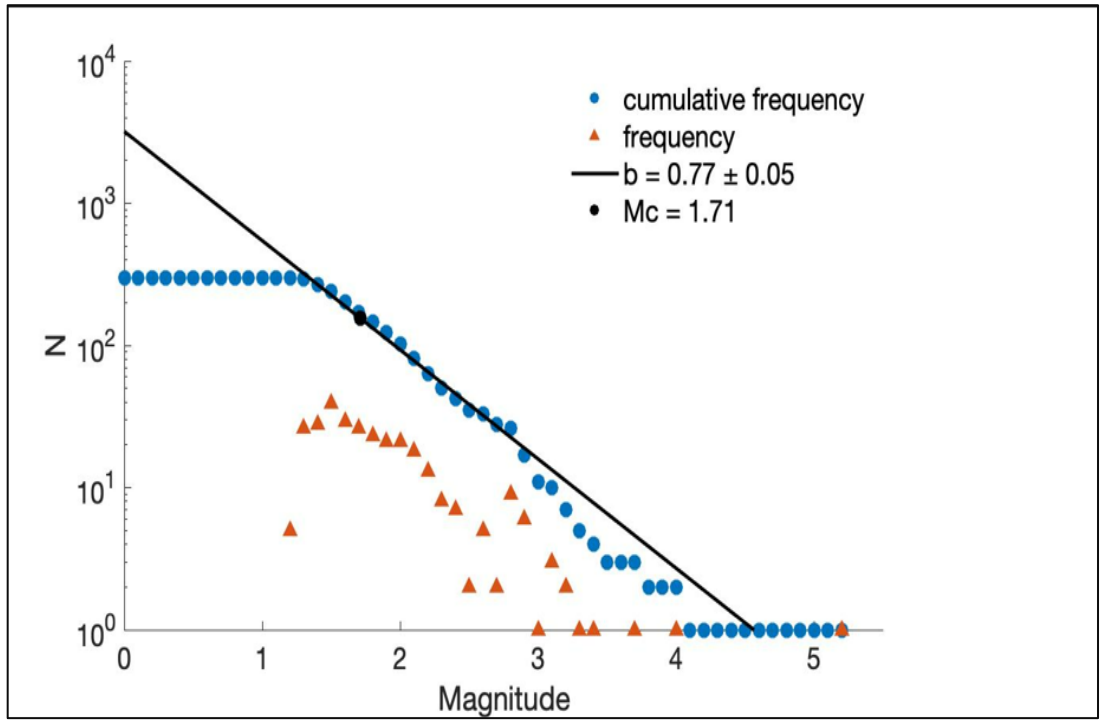

# Turkana-Karonga Comparison

## $M_L$=4.5 Turkana Sequence Omori's Law Decay Rate/ETAS model

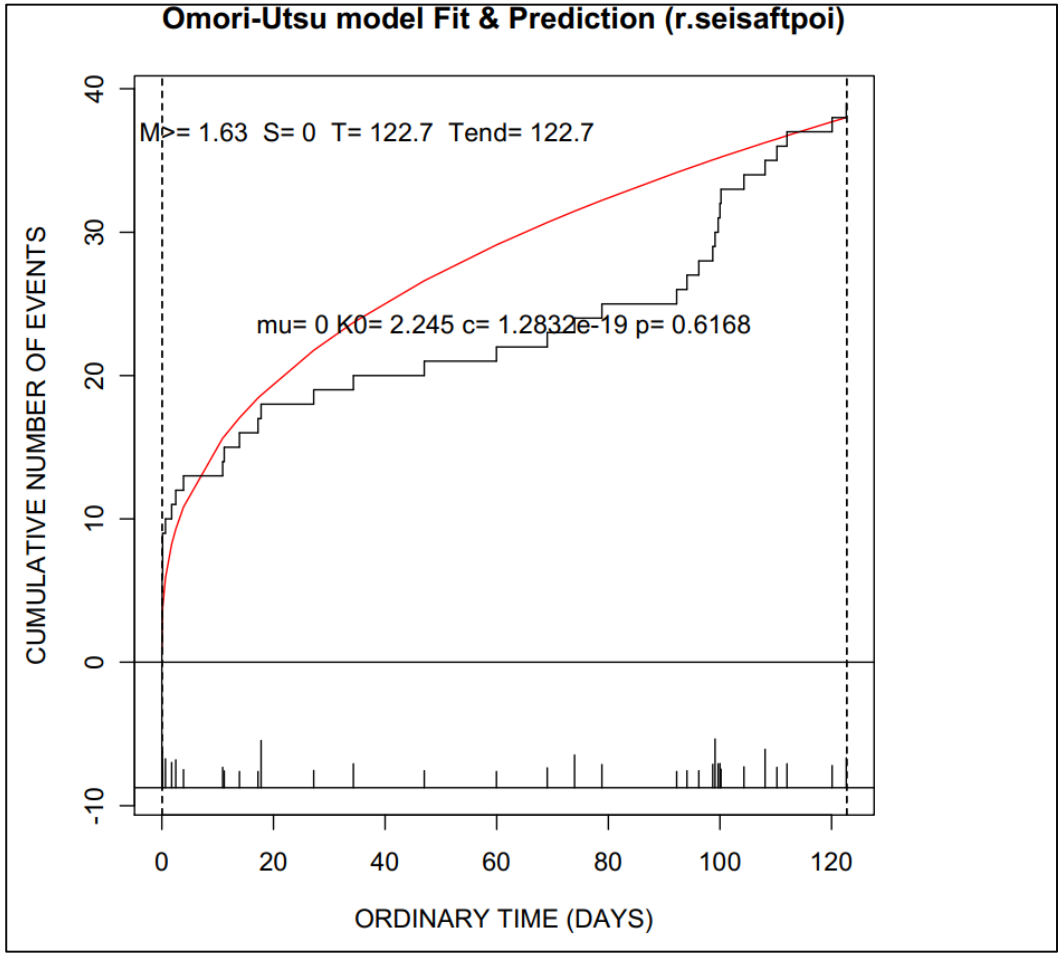


## $M_w$=5.2 Karonga Sequence Omori's Law Decay Rate/ETAS model

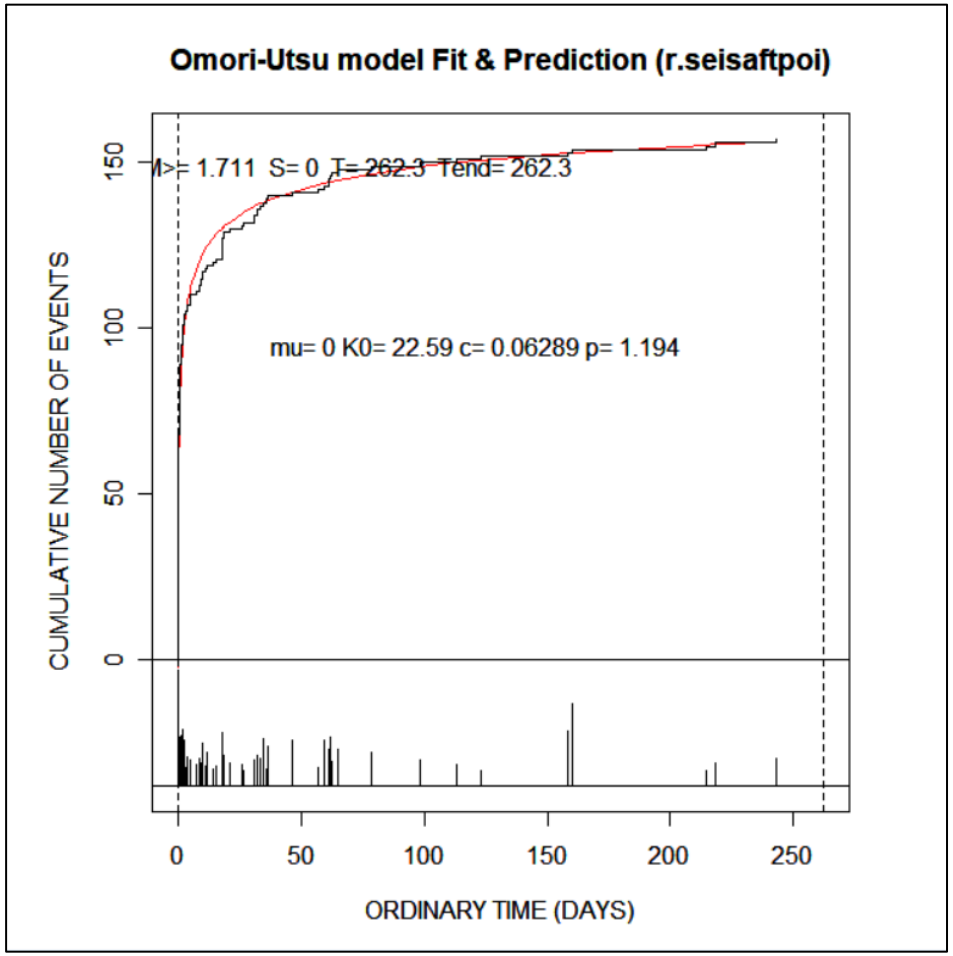

# Turkana-Karonga Comparison

## $M_L$=4.5 Turkana Sequence ETAS Model vs Transformed time

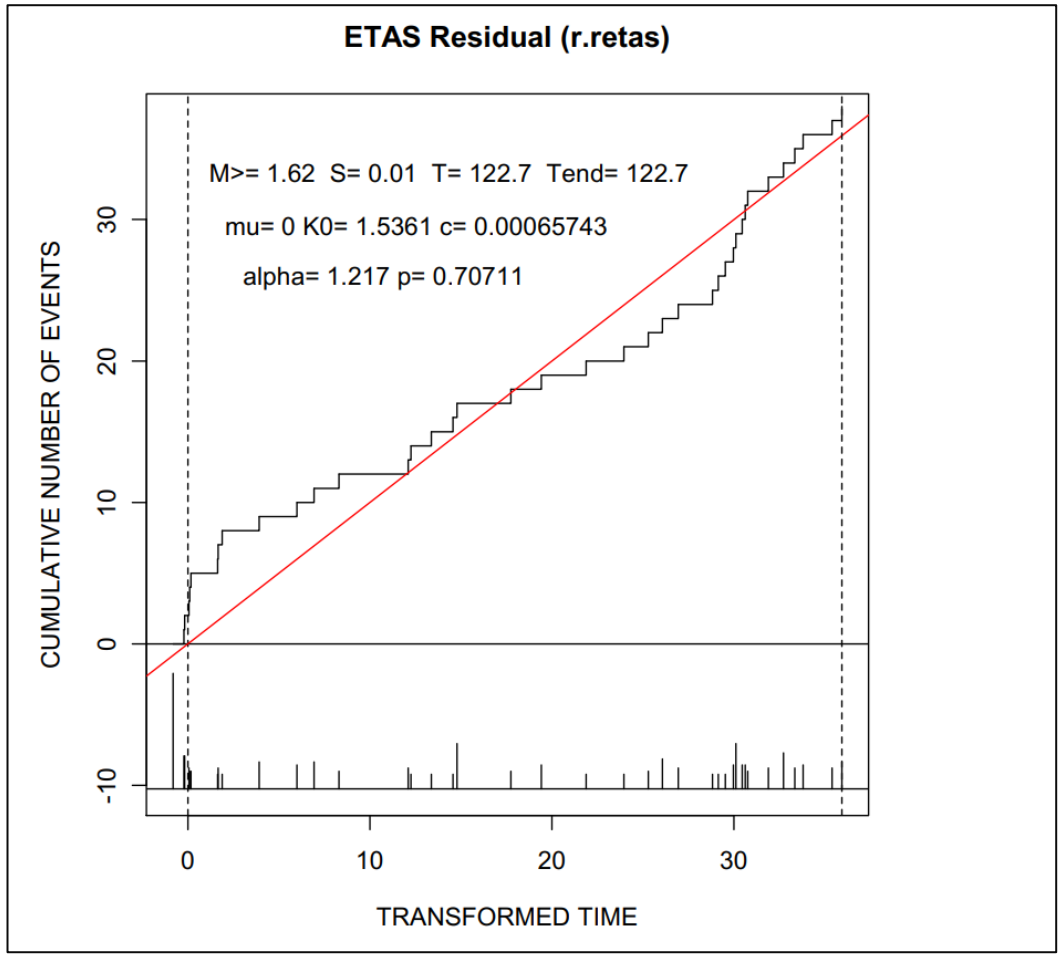


## $M_w$=5.2 Karonga Sequence ETAS Model vs Transformed time

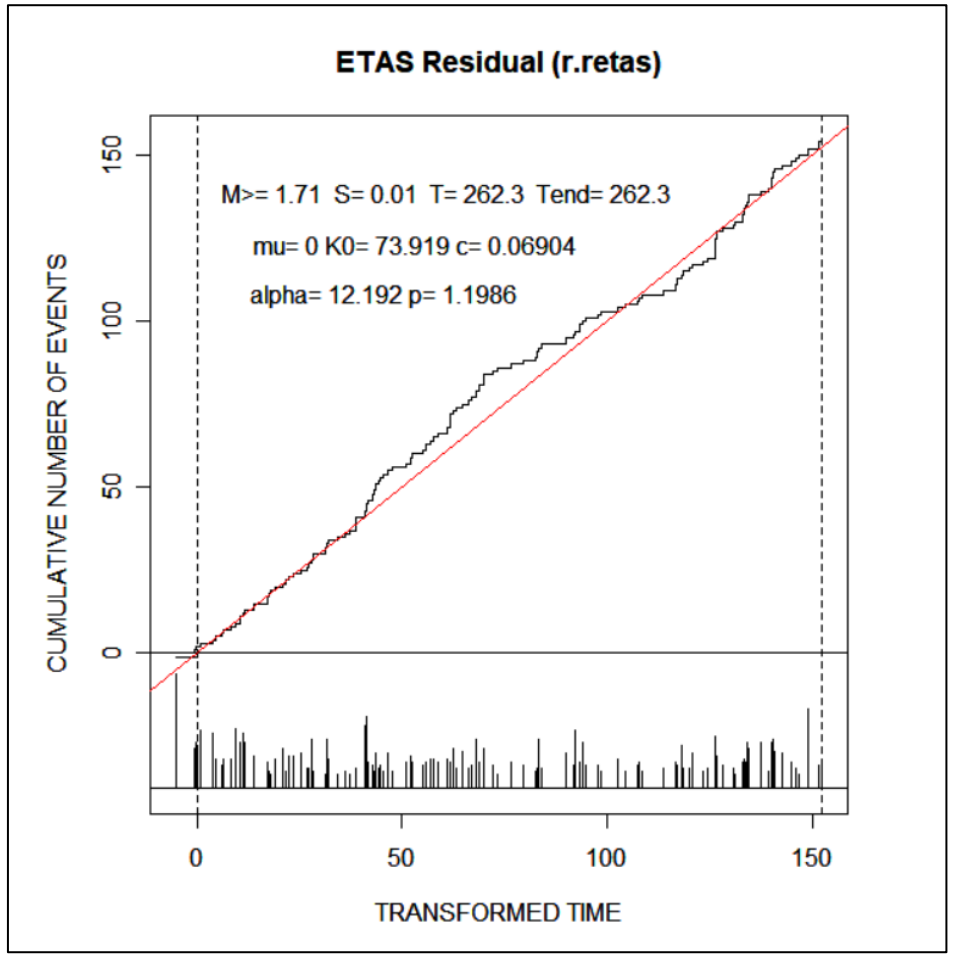

# Discussions

The $M_b$4.9 sequence was characterized by few aftershocks and a huge difference between the mainshock magnitude and the largest aftershock. Only two fault plane solutions of the largest aftershocks that were determined alongside the mainshock solution. The aftershocks are distributed along NNW-SSE normal fault plane (not purely normal fault plane, it has some oblique strike slip characteristic). Most of the aftershocks fall under Class 2 type of aftershocks, away from the main rupture plane but not large distance, in a distance approximately 3km in diameter along an approximately 8km long normal main rupture plane .

The aftershocks width can also be described as the fault zone width (Yukutake & Lio, 2017). Time-space distribution of the Turkana sequence in days indicates that most of the aftershocks occurred minutes and hours after the mainshock occurrence, though it is hard to show this distinction in seconds, minutes, and hours scale. The two aftershocks' fault plane solutions resonate with the main rupture plane solution towards the tip of the main rupture plane towards the north. The mainshock is located close to the tip of the main rupture towards the south in the distribution.

# Discussions Cont'd

The b-value for the Turkana sequence is high and this can be attributed to the big difference between the maximum aftershocks' magnitude and the mainshock magnitude, $M_L$=4.5; aftershocks < 3. A cut-off magnitude ($M_c$) of 1.62 is used to filter out events with magnitudes less than 1.62 to determine the parameter values of the ETAS model. Only 25 events meet this threshold and in return an unclear Omori-Utsu decay rate curve is produced. Similarly, the ETAS model parameters generated by this sequence are unique as compared to normal sequences where the population of aftershocks is large.

Based on a good spatial distribution of earthquakes in the region and good P- and S-wave models, Turkana Depression corroborates with the latter [Kounoudis et al., 2021]. Using the S- and P- wave arrival time residuals, one can explain the seismic anomalies caused by temperature variations in the mantle. Turkana Depression with a residual ( $\frac{\delta ts}{\delta tp}$ ) of 5.38 compared to maximum bounds thermal range of 3.6-3.8. This is indicative of high temperatures caused by mantle melt as a contributor to seismic variations as observed in this sequence [Kounoudis et al., 2021].

Magmatic and thermal-volatile fluids in the shallow crust may lead to aseismic deformation due to updip migration through sub-vertical faults below the surface. This may lead to strain partitioning hence low energy release and thus low magnitude aftershocks [Zheng et al., 2020]

# Discussions Cont'd

The rate of decay is similarly slow compared to a projected rate of ≥ 1. Considering some of the properties in this sequence such as low population of aftershocks, a huge difference between the maximum aftershock's magnitude and the mainshock magnitude, a high b-value, and the above model parameters, it can be attributed to a common seismic characteristic in the region which is probably magmatism.

# Discussions Cont'd

In a study done by Zheng et al., 2020, the $M_w$5.2 Karonga sequence is attributed to seismic and aseismic deformation caused by multiple faulting and fault intersections. The argument in this study these multiple fault intersections restrict deep seismic rupture propagation leading to strain partitioning. This strain is distributed across these multiple faults above 12 km. Additionally, hydrothermal fluids may have caused liquefaction through up-dip migration weakening the basement even further [Zheng et al., 2020].

On the other hand, there is no evidence of aseismic deformation nor fault intersections in the $M_L$4.5 Turkana sequence. Even though crustal anisotropy affects wavespeed variations and seismic heterogeneity at large, it is not a major contributor to the anomaly.

One of the major causes of seismic variations is thermal variation since temperature exerts more pressure on the uppermost mantle as compared to composition [Kounoudis et al., 2021].

# Discussions Cont'd

So, what could be the reasons behind the anomalies in Eliye Kink in Turkana?

Three possible reasons for the anomalies according to Zheng et al., 2020 findings are:

i. Degassing of volatile $CO_2$ implying Presence of petrographic anomalies in Eliye and Epir wells?

ii. Mantle melt -> Thermal fluid migration?

iii. Temperature variations due to upper mantle melt?

These three can cause strain partitioning hence low energy and few aftershocks of low magnitude order.

# Conclusions & Recommendations

## Conclusions

The Turkana sequence was characterized by low population events with magnitudes of the aftershocks being $M_L<3$ than the mainshock $M_L= 4.5$ which also resulted to a large b-value. This is due to magmatism, volatile fluid migration e.g., degassing $CO_2$ and temperature variations below the Turkana Depression caused by probable mantle plumes in the MER and EAR. The aftershocks were triggered off and along an impure normal NNW-SSE main rupture plane. The damage zones surrounding the main fault contain numerous subsidiary faults. There was no foreshock detected and background seismicity in the sequence.

The ETAS model generated from the Turkana sequence indicates a very low efficiency of an earthquake in producing an offspring event in this region. Also, the decay rate of these aftershocks is below a unit, which is an unusual value. This, however, indicates that there are no destructive aftershocks that are expected from a mainshock in this region at any given time. This is quite the opposite in Karonga region which indicates a high alpha value meaning a destructive offspring event can be produced if a large magnitude event occurs in the region.

The structural and tectonic setting of Turkana and Karonga are more distinct than similar. The former, which is confined in the eastern branch of the EARS, began its' formation between 45-30 Myr ago while the latter is confined in the southern segment of the western branch which began developing 13-12 Myr ago. For example, the mantle temperatures between the eastern and the western branches is about $100\text{-}150^0$ C underneath with eastern branch having a higher value (Hardarson, 2015).

# Recommendations

The two aftershocks' fault plane solutions determined in the Turkana sequence are not a representative of the wholesome subsidiary faults distribution. The multiple subsidiary faults distribution is characterized by different solutions since each aftershock is assumed to occur on its own minor fault surrounding the damage zone.

The rate of decay of the aftershocks is relatively poor and this can be attributed to low aftershocks population density. The best results for these two models, Omori's law on aftershocks decay rate and ETAS model, are achieved by high population densities in aftershocks. This is applicable in Equation 2 when determining the rate of occurrence of aftershocks at time, **t**.

More stations are needed to record the events to easily distinguish between an anthropogenic and natural sequence in a clear Omori's curve.

The comparison of these two sequences exhibit two distinct stages of rifting and volcanism. It is therefore non-comparative for the two ETAS models since each region is characterized by different slip deformation.

# References


Ambraseys, N., 1991. Earthquake hazard in the Kenya Rift: the Subukia earthquake 1928. *Geophys. J.Int.,* Volume 105, pp. 253-269.

Aslam, K. S. & Daub, E. G., 2018. Effect of Fault Roughness on Aftershock Distribution: Elastic Off-Fault Material Properties. *Journal of Geophysical Research: Solid Earth,* Volume 123.

Beauval, C., Hainzl, S., Scherbaum, F., 2006. Probabilistic seismic hazard estimation in low-seismicity regions considering non-Poissonian seismic occurrence. *Geophys. J .Int,* Volume 164, pp. 543-550.

Birhanu, Y., Bendick, R., Fisseha, S., Lewi, E., Floyd, M., King, R., Reilinger, R., 2016. GPS constraints on broad scale extension in the Ethiopian Highlands and Main Ethiopian Rift. *Geophysical Research Letters,* Volume 43, p. 6844–6851.

Boone, S. C., Kohn, B. P., Gleadow, J. W., Morley, C. K., Seiler, C., Foster, D. A., 2019. Birth of the East African Rift System: Nucleation of magmatism and strain in the Turkana Depression. *The Geological Society of America.*

Brune, S., Corti, G., Ranalli, G., 2017. Controls of inherited lithospheric heterogeneity on rift linkage: Numerical and analogue models of interaction between the Kenyan and Ethiopian rifts across the Turkana depression. *American Geophysical Union.*

Corti, G., Cioni, R., Franceschini, Z., Sani, F., Scaillet, S., Molin, P., 2019. Aborted propagation of the Ethiopian rift caused by linkage with the Kenya Rift. *Nature Communications.*

Dieterich, J., 1994. A Constitutive Law for Rate of Earthquake Production and its Application to Earthquake Clustering. *Journal of Geophysical Research,* 99(B2), pp. 2601-2618.

Ebinger, C. J., Keir, D., Bastow, I. D., Whaler, K., Hammond, J. O. S., Ayele, A., 2017. Crustal Structure of Active Deformation Zones in Africa:Implications for Global Crustal Processes. *American Geophysical Union.*

Ebinger, C.J., Bastow, I., 2018. *NSFGEO-NERC Collaborative Research: Turkana Rift Arrays to Investigate Lithospheric Strain (TRAILS),* s.l.: s.n.

Ebinger, C.J., Yemane, T., Harding, D.J., Tesfaye, S., Kelley, S., Rex, D.C., 2000. Rift deflection, migration, and propagation: Linkage of the Ethiopian and Eastern rifts, Africa. *Geological Society of America,* Volume 2, pp. 163-176.

Hollnack, D., Stangl, R., 1998. The seismicity related to the southerb part of the Kenyan Rift. *Journal of African Earth Sciences,* Volume 26, pp. 477-495.

Kagan, Y., 2002. Aftershock Zone Scaling. *Bulletin of the Seismological Society of America,* Volume 92, pp. 641-655.

Knappe, E., Bendick, R., Ebinger, C. J., Birhanu, Y., Lewi, E., Floyd, M., King, R., 2020. Accommodation of East African Rifting across the Turkana Depression. *American Geophysical Union.*

# References


Kounoudis, R., Bastow, I., Ebinger, C. J., Ogden, C. S., Ayele, A., Bendick, R., 2021. Body-Wave Tomographic Imaging of the Turkana Depression: Implications for Rift Development and Plume-Lithosphere Interactions. *Geochemistry,Geophysics,Geosystems*.

KRISP Working Group, 1991. Large-scale variation in lithospheric structure along and across the Kenya Rift. *Nature,* Volume 354, pp. 223-227.

KRISP Working Group, 1991. Large-Scale Variation in Lithospheric Structure along and Across the Kenyan Rift. *Nature,* Volume 354, pp. 223-227.

Liu, M., Stein, S., 2011. Earthquake, Aftershocks. pp. 192-194.

Maguire, P.K.H.,Shah, E.R., Pointing, A.J.,Cooke, P.A.V., Khan, M.A., Swain, C.J., 1988. The Seismicity of Kenya. *Journal of African Earth Sciences,* Volume 7, pp. 915-923.

Morley, C. K., Ngenoh, D.K., Ego, J.K., 1999. Introduction to The East African Rift. *AAPG Studies in Geology,* Volume 44, pp. 1-18.

Mulwa, J.K., Kimata, F., Suzuki, S., Kuria, Z.N, 2014. The Seismicity in Kenya (East Africa) for the period 1906-2010: A review. *Journal of African Earth Sciences,* Volume 89, pp. 72-78.

Mulwa, J., 2020. Earthquakes Occurrence on the East African Coast and Their Implication on Stress Drop along the Davie Ridge of the East African Rift System (EARS). *Universal Journal of Geoscience,* Volume 8, pp. 25-32.

Musila, M., Ebinger, C.J., Mariita, N., Bendick, R., Bastow, I., Aleye, A., Kianji, G., Nderitu, S.M., 2020. *Kinematics of linkage between the Main Ethiopian and Eastern rifts in the Turkana Depression.* s.l., AGU-iPostersSessions, p. 1.

Musila, M. et al., Submitted (2023). *Strain accommodation during continental rifting: Mantle lithosphere,* s.l.: s.n.

Mutegi, B., 2013. *Seismic Monitoring in Kenya,* s.l.: IRIS.

Ogata, Y., 1988. Statistical Models for Earthquake Occurrences and Residual Analysis for Point Processes. *Journal of the American Statistical Association,* 83(401), pp. 9-27.

Ogata, Y., 1998. Space-Time Point-Process models for earthquake occurrences. *Ann. Inst. Statist. Math.,* Volume 50, pp. 379-402.

Ogata, Y., 2006. *Statistical Analysis of Seismicity- Updated version (SASeis2006),* Tokyo: The Institute of Statistical Mathematics.

Omori, F., 1894a. On the After-shocks of Earthquakes. *J. Sci. Coll. Imp. Univ. Tokyo,* Volume 7, pp. 111-200.

Ostermeijer, G. S., 2019. *Multiscale High-Resolution Mapping of Fracture Damage Around Seismogenic Faults,* London: University College London.

Ozawa, S. & Ando, R., 2021. Mainshock and Aftershock Sequence Simulation in Geometrically Complex Fault Zones. *Journal of Geophysical Research: Solid Earth,* 126(e2020JB020865).

# References


Parsons, T., 2002. Global Omori law decay of triggered earthquakes:Large aftershocks outside the classical afterschock zone. *Journal of Geophysical Research,* Volume 107.

Pointing, A. J., 1985. *Seismicity and Lithospheric Structure of Northern Kenya,* 789 East Eisenhower Parkway: ProQuest.

Prodehl, C., Fuchs, K., Mechie, J., 1997. Seismic-refraction studies of the Afro-Arabian rift system- a brief review. *Tectonophysics,* Volume 278, pp. 1-13.

Prodehl, C., Mechie, J., Achauer, U.,Keller, G.R., Khan, M.A.,Mooney, W.D., Gaciri, S.J., Obel, J.D., 1994. The KRISP 90 seismic experiment-a technical revidw. *Tectonophysics,* Volume 236, pp. 33-60.

Purcell, P., 2017. Re-imagining and re-imaging the development of the East African Rift. *Tectonics and petroleum systems of East Africa.*

Ragon, T, Nutz, A, Schuster, M, Ghiene, J-F, Ruffet, G, Rubino, J-L, 2018. Evolution of the northern Turkana Depression (East African Rift System, Kenya) during the Cenozoic rifting: New insights from the Ekitale Basin (28-25.5 Ma).

Ray, M., 2002. Magmatism of The Kenya Rift Valley: A Review. *Earth and Environmental Science Transactions of the Royal Society of Edinburgh,* Volume 93, pp. 239-253.

Schofield, N., Newton, R., Thackrey, S., Watson, D., Jolley, D., Morley, C., 2021. Linking surface and subsurface volcanic stratigraphy in the Turkana Depression of the East African Rift system. *Journal of the Geological Society.*

Scholz, C., 1968. The Frequency-Magnitude Relation of Microfracturing In Rock and Its Relation to Earthquakes. *Bulletin of the Seismological Society of America,* Volume 58, pp. 399-415.

Scholz, C., 2015. On the stress dependence of the earthquake b value. *Geophysical Research Letters,* Volume 42, pp. 1399-1402.

Senior Seismic Analysis Committee, (SSHAC), 1997. *Recommendations for Probabilistic Seismic Hazard Analysis: Guidance on Uncertainty and Use of Experts,* s.l.: NUREG/CR-6372.

Smith, D. E. & Dieterich, J. H., 2010. Aftershock Sequences Modeled with 3-D Stress Heterogeneity and Rate-State Seismicity. *Pure and Applied Geophysics,* Volume 167, pp. 1067-1085.

# References


Stamps, S. D., Calais, E., Saria, E., Hartnady, C., Nocquet, J. M., Ebinger, C. J., Fernandes, R. M., 2008. A kinematic model for the East African Rift. *Geophysical Research Letters,* Volume 35.

Stein, S., Liu, M., 2009. Long aftershock sequences within continents and implications for earthquake hazard assessment. *Nature,* Volume 462, pp. 87-89.

Tongue, J., Maguire, P., Burton, P., 1994. An earthquake studyin the Lake Baringo basin of the central Kenya Rift. *Tectonophysics,* Volume 236, pp. 151-164.

Utsu, T., Ogata, Y., Matsu'ura, R. S., 1995. The Centenary of the Omori Formula for a Decay Law of Aftershock Activity. *Journal of Phys. Earth,* Volume 43, pp. 1-33.

Utsu, T., 1970. Aftershocks and Earthquake Statistics (I)- Some Parameters which characterize an Aftershock Sequence and their Interrelations. *Journal of the Faculty of Science, Hokkaido University, Japan Series 7,* Volume 3, pp. 129-195.

Utsu, T., 1971. Aftershocks and Earthquake Statistics (II)-Further Investigation of Aftershocks and Other Earthquake Sequences Based on a New Classification of Earthquake Sequences. *Journal of the Faculty of Science, Hokkaido University, Series 7, Geophysics,* 3(4), pp. 197-266.

Utsu, T., 2002. Statistical Features of Seismicity. *International Handbook of Earthquake and Engineering Seismology,* Volume 81A, pp. 719-724.

Weimer, S., Wyss, M., 2002. Mapping spatial variability of the frequency-magnitude distribution of earthquakes. *Advances in Geophysics.*

Young, P.A.V., Maguire, P.K.H., Laffoley, N. d'A., Evans, J.R., 1991. Implications of the distribution of seismicity near Lake Bogoria in the Kenya Rift. *Geophys. J. Int.,* Volume 105, pp. 665-674.

Yukutake, Y. & Lio, Y., 2017. Why do aftershocks occur? Relationship mainshock rupture and aftershock sequence based on highly resolved hypocenter and focal mechanism distribution. *Earth, Planets and Space.*

Zheng, W., Oliva, S. J., Ebinger, C. & Prirchard, M. E., 2020. Aseismic Deformation During the 2014 Mw5.2 Karonga Eathquake, Malawi, From Satellite Interferometry and Earthquake Soure Mechanisms. *Geophysical Research Letters.*

Zielke, O. & Strecker, M. R., 2009. Recurrence of Large Earthquakes in Magmatic Continental Rifts: Insights from a Paleoseismic study along Laikipia-Marmanet Fault, Subukia Valley, Kenya Rift. *Bulletin of The Seismological Society of America,* 99(1), pp. 61-70.